

Lausanne, octobre 2013

Projet de semestre M1 Automne 2013

Candidat : PICARD Cyril
Section de Génie Mécanique

Sujet : Control System for Babyfoot

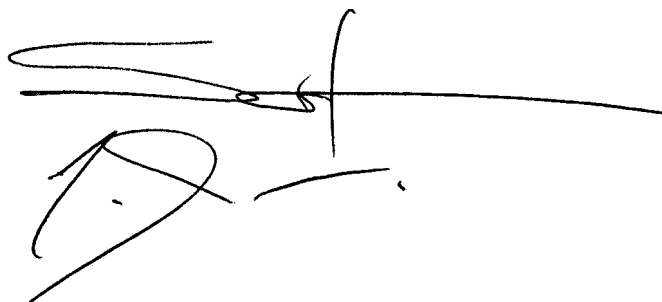
The aim of this project is to improve the existing control of the bar that holds the players. The control strategy should use the ball measurements and implement first a solution that is able to reliably stop the ball, then design the control strategy that is able to shoot in the opponent's goal. Finally design a simple strategy to pass the ball among players of the same team but in different bar

Le nombre de crédits réservés au plan d'études pour ce projet est de dix.

Dr. Christophe Salzmann
Prof. Colin Jones

Assistants responsables

KORDA Milan (tél. int. 3 10 59)
GORECKI Tomasz (tél. int. 3 42 20)





Abstract

From the required mechanical changes to the setup that has been chosen to control multiple bars of an automated foosball, this document is an overview of the work made during the 3rd project on the automated foosball focusing on control. The modeling and identification of the dynamics is given an important part and used to design effective controllers. Play strategies are presented in a state-machine approach. At last, some practical information on how to use the LabView interface is given the appendix.

Contents

Abstract	iii
List of figures	vi
List of tables	vii
1 Introduction	1
2 Mechanical redesign	3
2.1 Tracking the failure	3
2.2 Corrected design	3
2.2.1 Adding degrees of freedom	4
2.2.2 Stabilizing the rotation motor	5
2.2.3 Summary and final corrections	5
2.3 2nd actuator	5
3 Control setup	7
3.1 Brushless motor drives	8
3.1.1 Rotation motor drive configuration	9
3.1.2 Translation motor drive configuration	9
3.2 Acquisition chain	9
3.3 Power supply selection	10
3.4 Coordinate system and naming convention	11
3.5 LabView structure	12
4 Identification and controller design	13
4.1 Identification	13
4.1.1 Player rotation system	13
4.1.2 Player translation system	17
4.2 Controller design	19
4.2.1 Rotation axis controller	20
4.2.2 Translation axis controller	20

Contents

5	Play strategies	23
5.1	General sequences	23
5.1.1	Initialization	23
5.1.2	Shoot	23
5.2	Implemented strategies	24
5.2.1	Track & shoot	24
5.2.2	Collaborative track & shoot	26
6	Conclusion	27
A	Mechanical parts order	29
B	LabView interface manual	31
C	Drawings	35
	Bibliography	51

List of Figures

2.1	Sketch of possible repair using a double universal joint	4
2.2	Assembly drawing of the corrected design for the mounting of the rotation motor	5
3.1	Overview of the control setup	7
3.2	Current measured in the translation motor during a "standard" track and shoot operation mode.	10
3.3	Coordinate system used across the project	11
4.1	Synthetic visual representation of the rotation axis model	13
4.2	Response of the rotation system to a step input.	14
4.3	Response of the rotation system to a step input with both the true model and the theoretical model with $J = 3.7 \cdot 10^{-4} [kgm^2]$, $M_f = 0.00001 [Nms]$ and $K_m = 0.0192 [Nm/A]$ (as specified by maxonmotor).	15
4.4	Bode diagram of the theoretical model, the identified model and the result of the Fourier analysis on the rotation system.	16
4.5	Comparison of the two identified models against measured data for a shoot (without ball).	16
4.6	Bode diagram with the result of the Fourier Analysis, the theoretical model and the model identified by using an output error structure.	18
4.7	Response of the translation axis to a sequence of steps and comparison with two models	19
4.8	Validation of the designed controller for the rotation axis.	20
4.9	Validation of the designed controller for the translation axis.	21
5.1	Shoot subsequence state machine representation	24
5.2	Track & shoot algorithm state machine representation	25
5.3	Track & shoot sequence when looking at the translation motor comparing the reference and the actual position	26
B.1	Main VI setup interface	33
B.2	Main VI control interface	33

List of Tables

3.1	Summary of the settings used to configure each ESCON box.	8
3.2	Symbols used to study the system and their description	11
A.1	Ordered mechanical parts	29
A.2	Ordered parts for the structure (from item24)	30
B.1	List of all LabView VIs and their description	32

1 Introduction

As my first Master semester project, I decided to get back to a project I had already worked on as a project during my Bachelor: the automated foosball. As semester projects are quite short compared to all the time constraints linked to the design of a new mechanical system and its control, students don't often get a chance to see their system in action and to be able to realize what necessary hypothesis proved to be accurate and those that don't. So for me, being able to get back to a mechanism I have co-worked on is an motivating thought.

During the last semester, two different projects worked on the automated foosball: one to enhance the control and the other to add eyes to the system. After the summer break, five students have tried to tackle the problems still remaining. My project was focusing on enhancing the current mechanical design, which time had proven to be fragile, to integrate the position of the ball as measured by the camera into the control scheme and to work on play strategies. To achieve this, I have worked in close collaboration with Guillaume Clivaz, which has been working on the "vision" part this semester.

This report aims to walk the reader through all information required to understand the current design and be able to work on its improvements. It starts by covering the mechanical aspects to show what might have been the cause of the motor failure and which solutions were selected. It then continues by detailing the acquisition chain, the configuration of the motor drives and the imagined structure for the LabView program. The modeling of the system and the design of the controllers is given an important part, before going over the implemented play strategies.

Even though this document tries to be comprehensive, the reader should be familiar with the current mechanical design and setup to understand the notions presented in this report. If needed, further details can be obtained from the previous reports.

2 Mechanical redesign

At the start of the project, the actuator was not working. The rotation motor had broken into two pieces between the gearbox and the motor itself. A new motor had already been ordered during the summer but before putting it back to work, it was necessary to identify the cause of the malfunction and take corrective measures.

2.1 Tracking the failure

From a first visual analysis, one could notice that the gears had ground themselves (even though the original plastic gears had already been replaced by metal ones) and that the threading linking the gearbox with the motor was worn out. Further disassembly of the rotation axis structure showed that the ball bearing suffered strong radial efforts and the screws holding the motor to the carriage had loosened up.

With these points in mind and after consulting the ATME workshop, two possible issues could be identified:

- With the new rigid link between the system and the foosball bar, all vibrations and misalignments of the axis of the bar and the one of the motor result directly in radial stress on the shaft of the gearbox. These small gearbox are not designed to handle large forces (max. permissible radial loading 25 N).
- The rotation motor is, conforming to maxon recommendations, only linked to the moving carriage by the 6 screws at the level of the gearbox. It now seems clear that maxon is not expecting its motors to be mounted on parts with high dynamics, not even mentioning that the weight of the motor is high compared to other parts.

2.2 Corrected design

Having now identified these issues, I have worked on:

Chapter 2. Mechanical redesign

- adding degrees of freedom between the foosball bar and the shaft of the motor to reduce the radial stress
- adding support to the same motor further away from its fixation point to reduce the inertial efforts on the threading linking the gearbox to the motor

This mechanical redesign has to follow these constraints:

- minimize the amount of mechanical parts to machine
- minimize the weight of the mobile parts
- fit within the size limits of the current design

With these aspects in mind, the following subsections develop the different possible solutions and finally, detail the selected option.

2.2.1 Adding degrees of freedom

The idea is to decouple all the movement of the foosball bar except for the rotation around its axis from the shaft of the motor. In the previous design, the only ball bearing would tolerate some movements but worked also as a lever and could thus amplify the efforts.

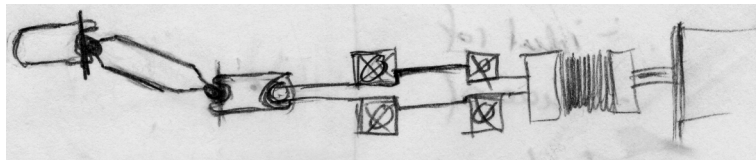


Figure 2.1: Sketch of possible repair using a double universal joint

To remove all stress on the shaft of the motor, the ideal solution (Figure 2.1) would be to add a double universal joint connected to the foosball bar followed by a two-ball-bearing-supported axis linked to the shaft of the motor through a flexible coupling (torsionally stiff). This would also be the most stable solution, but it requires a great number of new parts and would significantly increase the weight and the complexity of the system. Plus, under high dynamics, it is not clear whether the double universal joint might not bend the foosball bar.

A more compact solution would get back to a single-ball-bearing-supported axis, but would use a flexible coupling on the motor side and a single universal joint on the other side. After many discussions and analysis of the uneven movement of the tip of the foosball bar, the advantage of the use of a universal joint versus its weight is not significant enough.

A bigger ball bearing with a flexible coupling has been chosen as the solution. The flexible coupling is dimensioned based on the available size, even though the maximum permissible

torque (2 Nm) might be exceeded briefly when trying to shoot the ball at full power or when the players get blocked by the ball. It is difficult to evaluate the risk linked to this, as the high torques will usually last less than a second and as future experimentations have shown, the tightening of the flexible coupling to the shaft might not even be strong enough to transmit such efforts (and would slip instead). Considering the relatively small price (~50 CHF) of this part, this uncertainty is considered acceptable.

2.2.2 Stabilizing the rotation motor

Considering the geometry of the carriage and the way to motor is linked to it, it appears that one effective way to stabilize the motor is to add a cylinder around the motor and to use some polymer in between to damp the vibrations and oscillations. To fit within the available space, the supporting cylinder is chosen quite thin and a simple O-ring joint is used to transmit the effort from the movement of the motor to its case. It was also decided to add glue to the six screws holding the motor to the carriage.

2.2.3 Summary and final corrections

The selected solution to correct the current design is shown on Figure 2.2. It includes a flexible coupling and a cylindrical support with an O-ring joint for the motor.

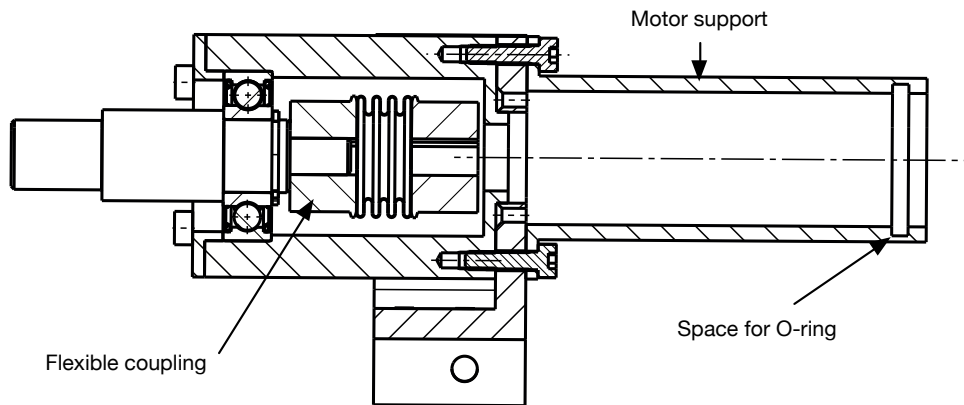


Figure 2.2: Assembly drawing of the corrected design for the mounting of the rotation motor

2.3 2nd actuator

In order to implement some strategy algorithms involving controlling two rows of players, a 2nd actuator based on the same design has been produced. A part from implementing the corrections detailed previously others aspects have been changed and are listed below:

Chapter 2. Mechanical redesign

- The ball bearings, the pulleys, the timing belt have been ordered at Mädler (instead of Rollin SA), often cutting the price by a factor two, for the same quality.
- The NSK linear guide has been replaced by a MiSUMi linear guide. The shipping delay of the first was of 6 months. The change affects these mechanical parts: the main support and the carriage.
- The item24 structure is now using mainly Automatic-Fastening Sets (more stable) to realize right angle links between two structure elements.

The full list of all parts that has been ordered is visible in Tables A.1 and A.2 (Appendix A). The drawings for all parts can be found in Appendix C.

3 Control setup

This chapter aims to discuss the control chain from the way the motors are connected to the computer to the chosen structure for the LabView VI, through the selection of the power supplies and the used coordinate system. Figure 3.1 illustrates the whole infrastructure and shows the principal options of each stage.

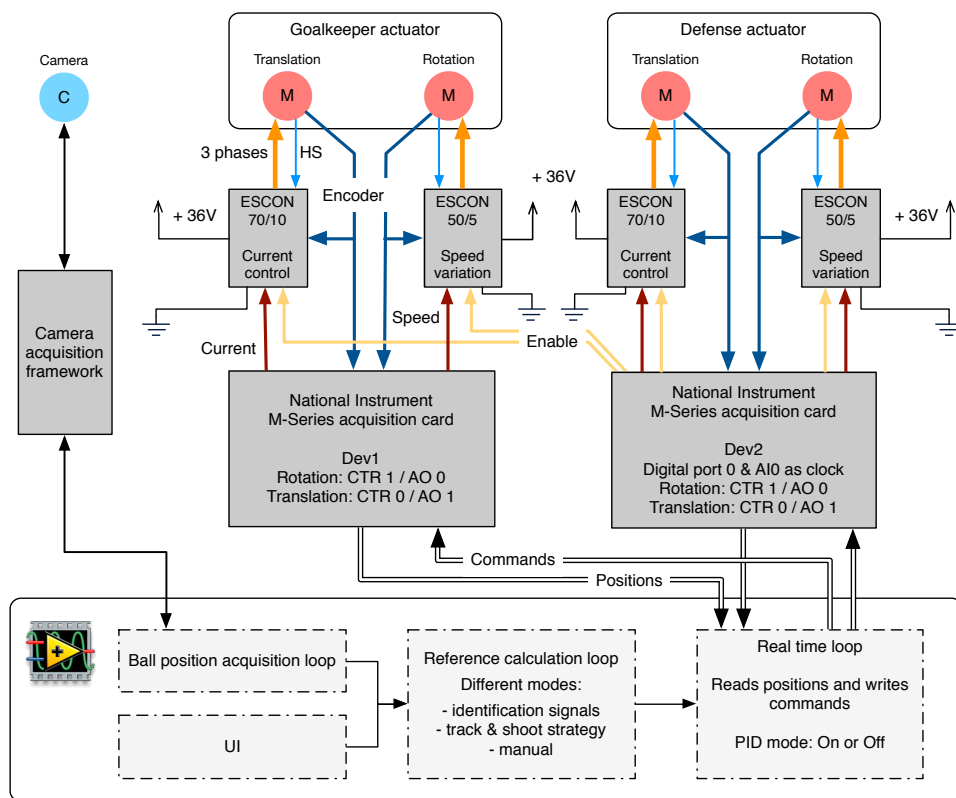


Figure 3.1: Overview of the control setup

3.1 Brushless motor drives

The drives are essential to power brushless motors, where the electronic is used to switch phases according to the position of the rotor as sensed by the hall sensors. The first Homofaber project chose to use the ESCON 50/5 box designed by maxonmotor. One ESCON can drive one motor. Compared to previous projects on the foosball, the ESCON for the translation motor was replaced by the newer ESCON 70/10. This enables the translation motor to be powered by up to 30A for peak performances and to be able to provide the nominal current (6.79A).

These ESCONs are connected to the motors as shown in their manual. Once connected, they need to be configured through the ESCON Studio software (only available on Windows). There, one needs to set some constants of the motor. One can then choose the operation mode and configure the inputs and outputs. There are three operation modes available: current control, speed control (closed loop), speed control (open loop). The last mode is the only open loop mode, as the two others have an internal feedback loop. The internal controller can be either automatically tuned or manually through two parameters: the static gain and the integral time constant. For each mode, additional parameters can be configured (current limitation, IxR compensation mode, speed ramp, offset,...) and if needed, the reader should have a closer look at the available documentation for these drives.

It is important to note that these ESCONs definitely add non-linear dynamics to our system. For instance, based on the thermal time constant of the windings, it determines whether it can apply the maximum current or only the nominal current, affecting the performance. But for the same reason, they also add security.

Table 3.1: Summary of the settings used to configure each ESCON box.

Settings	Value
ESCON 50/5 – rotation motor	
Regulator mode	current control
Regulator	Auto-tuning
Current limit	15A
Set value	Analog input map -10V to 15A map 10V to -15A
ESCON 70/10 – translation motor	
Regulator mode	open loop speed control Adaptive IxR
Regulator	Auto-tuning
Current limit	30A
Set value	Analog input map -10V to 16700rpm map 10V to -16700rpm
Ramp	none

3.1.1 Rotation motor drive configuration

To be able to finely control the power delivered by the rotation motor during a shoot, its ESCON is set to current control mode. The internal controller has been tuned with the Auto-tune mode. The current limit is set to $\pm 15A$, which is the maximum allowed. The current set value is an analog input where $\pm 10V$ is matched to $\mp 15A$ (sign inversion to make the rotation clockwise when the input is positive). Then, there is also a digital input "Enable" which controls whether the motor is enabled or not.

3.1.2 Translation motor drive configuration

The drive for the translation motor is set to open loop speed control. At first, similarly to the rotation motor, the current control mode has been tested. The idea behind the choice of current control is to be able to apply a feedforward which corresponds to the static friction of the translation system (being quiet important) and thus get rid of this non-linearity.

Even though this setup appears interesting on the paper, its application proved to be unstable close to the desired reference position, as the motor would oscillate around this point at high frequency. Adjusting the parameters of the controller would never remove all oscillations. This was also true for even more complex solutions such as a dead band or a low-pass filter on the command.

The nature of the instability was also affected by changes to the ESCON current controller, indicating that the issue is a combination of multiple effects: the dynamics at high frequencies of the belt and the not so predictable behavior of the ESCON drive current controller. David Ingram, PhD at the laboratory, suggested that using a third pulley to create the tension in the belt (instead of using one of the two) would help reduce this problem. Due the configuration of the actual system, it is not easily applicable and was thus not tested during this project. Changing the drive to open loop speed controlled finally helped to get rid of the oscillations.

In this mode, the current limit is set to $\pm 30A$. The set value is read from an analog input which matches $\pm 10V$ to ∓ 16700 rpm. The motor can be enabled through a digital input.

3.2 Acquisition chain

As shown in Figure 3.1, for each motor the LabView interface writes an analog value (the command), a digital value (enable switch) and reads the position from an encoder (only channels A and B are connected). A part from these ports, the LabView interface also starts an analog input acquisition (only one for all motors), which serves as a precise clock for the real-time loop.

As the used M-series acquisition cards only have two counters (encoder reader ports), the control of two actuators requires the use of two acquisition cards. For more convenience, the

counters and the analog outputs are used from the same card for each actuator, but all digital outputs are connected to *port0* of one of the acquisition cards (*Dev2*).

The speed of the motor could be acquired from the ESCON as an analog value, but previous projects used it and it proved to be quiet noisy. Instead, the speed is now calculated by deriving the position. The results are good for the rotational speed, but needed to be improved by filtering for the translation. Equation (3.1) represents the 1st order filter used.

$$H_s(z) = \frac{0.1342z}{z - 0.8658} \quad (3.1)$$

3.3 Power supply selection

With the increasing number of actuators and the increase of power allowed by the use of the ESCON 70/10, a strong power supply (or power supply network) is needed and would replace the currently used KEPCO.

Based on the available power supplies on the market, it is economically not necessarily interesting to acquire one big power supply to power all motors (up to 16 if all bars are controlled). Considering that not all bars will shoot at the same time, having one power supply of approximatively 15 to 20A (at 36V) would be enough to power all rotation motors (for the actual design with an ESCON 50/5 drive).

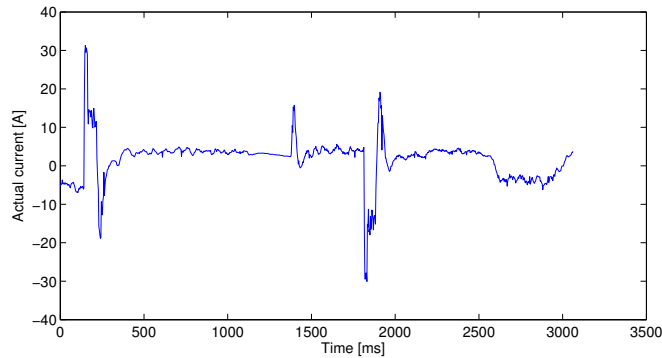


Figure 3.2: Current measured in the translation motor during a "standard" track and shoot operation mode.

For the translation motors the question is more complex, as in theory, to be able to go to the limit of the ESCON 70/10 drive, a 30A power supply is needed for every motor. Measures show (Figure 3.2) that during short period of time the current does go up to 30A, but note that the KEPCO (used in this test case) rated for 12A was able to follow the demand (maybe taking advantage of breaking energy). All these information should be taken into account when choosing the right power supply (supplies).

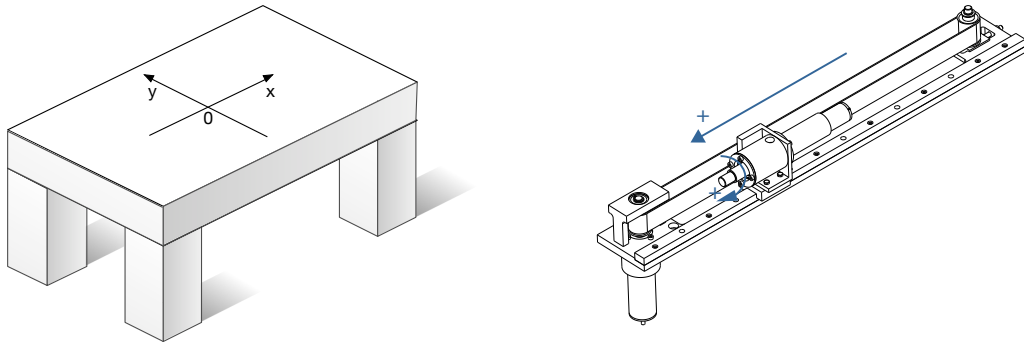
3.4. Coordinate system and naming convention

Francis ordered a more compact power supply rated for 36V and 29.5A for the rotation motors, but it did not handle well the excess of energy when changing the direction of rotation and the use of a Zener diode did not help solve this issue. It is probably required to install a capacitor (quite big) or a shunt. Due to a lack of time, the power supply of the kite project was temporarily used.

3.4 Coordinate system and naming convention

This section introduces the coordinate system and the naming convention that is used through out the next chapters and in the LabView controller.

Figure 3.3 shows the axis convention and their positive direction for the position of the ball and for the position of the system in rotation and translation.



(a) X and Y axis and their positive direction used to position the ball (b) Positive direction for the translation and rotation motors

Figure 3.3: Coordinate system used across the project

Table 3.2: Symbols used to study the system and their description

Symbol	Description
θ_m	Angular position of the rotation motor. The current angle when the system is started, is considered to be position 0
θ_p	Angular position of the players. It is link to θ_m by the following formula: $\theta_m = r_{rm}\theta_p$
r_{rm}	Ratio of the gearbox of the rotation motor.
J	Moment of inertia of one bar and all the parts in rotation connected to it.
J^*	Same moment of inertia as seen by the motor: $J^* = J/r_{rm}^2$.
ϕ	Angular position of the translation motor.
r_{tm}	Ratio of the gearbox of the translation motor.
I	Moment of inertia of one bar when considered in translation as seen by the motor. $I = m\left(\frac{D_{pulley}}{2}\right)^2 \frac{1}{r_{tm}^2}$
θ_c	Reference angular position.

3.5 LabView structure

In this last section of the chapter, some aspects of the LabView structure are described. Compared to the previous version of the LabView program (V1, V2 and V2.1), version 3, which was created this semester, is a full rewrite with the goal to integrate the ball tracking system (project "Vision") and to develop a multi-bar-ready software.

A part from the initialization part (creation of the required variables, acquisition setup,...) and the end part (writing data, closing acquisition), there are now five loops running in parallel. The idea was to reduce the complexity of the time-critical loop (called real-time loop) and to move the other tasks into separate loops to set their running rate individually. Thus, the five loops are:

1. the real-time loop, which acquires the position, calculates the command (controller) and writes the command
2. the ball position acquisition loop
3. the reference calculation loop, which based on the current operation mode generates the reference positions
4. the display loop, which processes the data from the real-time loop to display it on graphs (or save it)
5. the event loop, which reacts to changes made in the user interface

One reference is composed of an identifier (ID), two arrays with all the successive set values (one for the rotational and one for the translational position), two booleans indicating whether to use the controller or not and two pointers that are only used by the real-time loop to keep track of the current set value to consider in the array. Each actuator receives its one reference.

There are two points that are worth mentioning concerning these references:

- The identifier is used to notify the real-time loop that it is a new reference (when different then the previous one) and that the pointers should be reset to 0.
- The booleans are used to choose between open loop (false) and closed loop (true). When in open loop mode, the set values are directly used as commands.

Once the command has been calculated, it goes through a saturation. One reason for this is to respect the given limits of the ESCON and of the acquisition card (10V). Plus, for the rotation motor, the saturation was empirically reduced to 14A (instead of 15A) to limit the over current in the winding of the motor when in breaking mode, which would otherwise trigger a security in the ESCON.

4 Identification and controller design

4.1 Identification

To be able to design a controller for the actuator and to help for further works on the system, this chapter is presenting the models that represent the dynamic of one actuator (the bar with two players to be precise). In this analysis, the two axis (translation and rotation of the players) are taken into account separately as they are independent.

Throughout this chapter, the sampling time is taken as $T_s = 1\text{ms}$.

4.1.1 Player rotation system

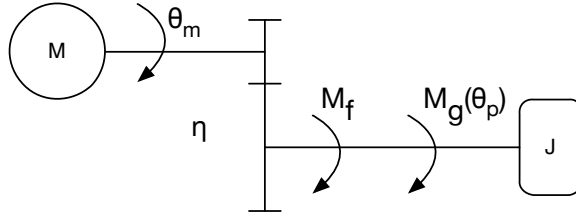


Figure 4.1: Synthetic visual representation of the rotation axis model

As a primer to the identification, a model can be derived from the physics of the system. Figure 4.1 is representing the considered system: M_f is a viscous friction momentum, M_g is the momentum created by the gravity on the players, K_m the torque constant of the motor. Other symbols are described in Table 3.2. For this axis, Newton's law is formulated as shown in Equation (4.1).

$$J^* \ddot{\theta}_m + M_f \dot{\theta}_m + M_g \sin(\theta_p) = K_m i \quad (4.1)$$

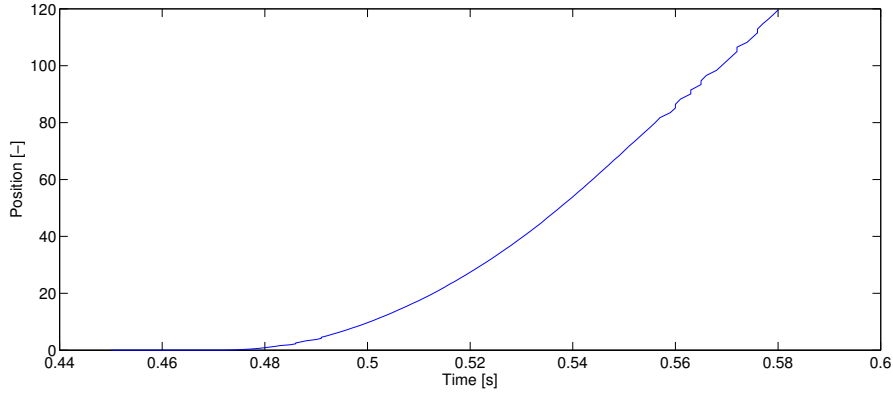


Figure 4.2: Response of the rotation system to a step input.

The M_g parameter is quite difficult to identify because of a lack of information on the precise geometry and weight of the parts (players). When looking at the step response of the system (Figure 4.2), this gravity term, with the effect of \sin would create oscillations in the position, but no such oscillations can be seen. From this, I deduce that M_g is much smaller than the other parameters. Therefore, the effect of gravity is neglected. Then, taking the Laplace transform and considering the position θ_m as the output and the current i as the input, the system can be represented by Equation (4.2).

$$G_r(s) = \frac{\Theta_m(s)}{I(s)} = \frac{K_m / J^*}{s(s + M_f / J^*)} \quad (4.2)$$

$$G_r(z) = \frac{J^* K_m}{M_f^2} \frac{(-1 + \frac{M_f}{J^*} + \exp(-\frac{M_f}{J^*} T_s))z + 1 - (1 + \frac{M_f}{J^*} T_s) \exp(-\frac{M_f}{J^*} T_s)}{z^2 - (1 + \exp(-\frac{M_f}{J^*} T_s))z + \exp(-\frac{M_f}{J^*} T_s)} \quad (4.3)$$

As suggested by [2], the design of a numerical controller should be made based on the discretized model of the system. Using equation (5.1) from the previous, one can calculate the discretized transfer function, which is then given by Equation (4.3).

This model based on physical considerations remains still quite theoretical, mainly as it is very difficult to correctly estimate *a priori* M_f , the friction parameter. By manually adjusting the M_f parameter (as well as J) in MATLAB, I have been able to get a good match of the step response previously shown. Figure 4.3 shows the true response with the simulated response.

The two responses start to separate around $t = 0.56s$. If looking at the derivative of the position, one would notice that the speed saturates at $\dot{\theta}_m = 16000$ rpm after this time for the true system – very close to the nominal speed of the motor. This non-linear effect is, by the nature of the analysis, not taken into account. Replacing the constants in (4.3) by their numerical values,

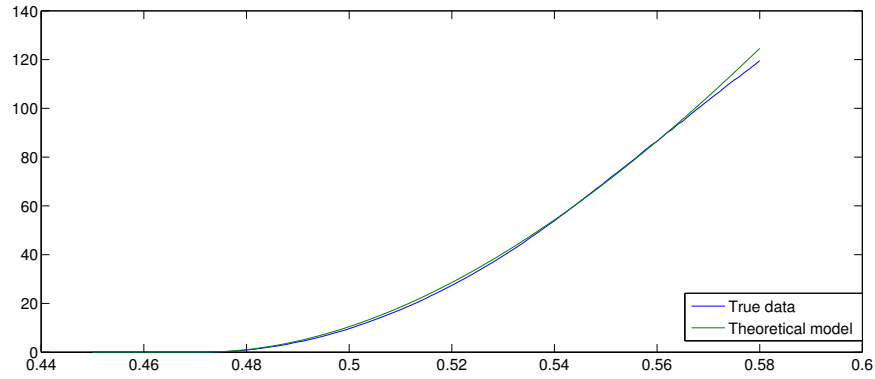


Figure 4.3: Response of the rotation system to a step input with both the true model and the theoretical model with $J = 3.7 \cdot 10^{-4} [kgm^2]$, $M_f = 0.00001 [Nms]$ and $K_m = 0.0192 [Nm/A]$ (as specified by maxonmotor).

one gets Equation (4.4).

$$G_r(z) = \frac{0.006627z + 0.006612}{z^2 - 1.993z + 0.9931} \quad (4.4)$$

To validate that there are no other dynamics that are significant and that have been omitted, a more conventional identification process is also applied. Following [1] and using an output error structure, a discrete transfer function of the system is identified. An MLS signal (close to a PRBS) is used as excitation.

The result of this work is shown in the frequency domain on Figure 4.4. Equation (4.5) shows the identified transfer function using an output error structure. It is similar to the theoretical model.

$$G_{roe}(z) = \frac{-0.002037z + 0.01385}{z^2 - 1.9921z + 0.9921} \quad (4.5)$$

To determine which model is better, they were tested against measured data. The applied command (current set value) and the position of the system was recorded during a shoot and the position was simulated on the two models applying the same command (Figure 4.5). The theoretical model offers a better fit and is almost able to predict correctly the full move, although the command applied is not trivial (steps, sines). The models fail to get the players back to zero. The most possible explanation is that the truly applied current is different for the set value given to the ESCON drive (see Subsection 3.1.2). Further investigation of this is required, but is not performed in this report.

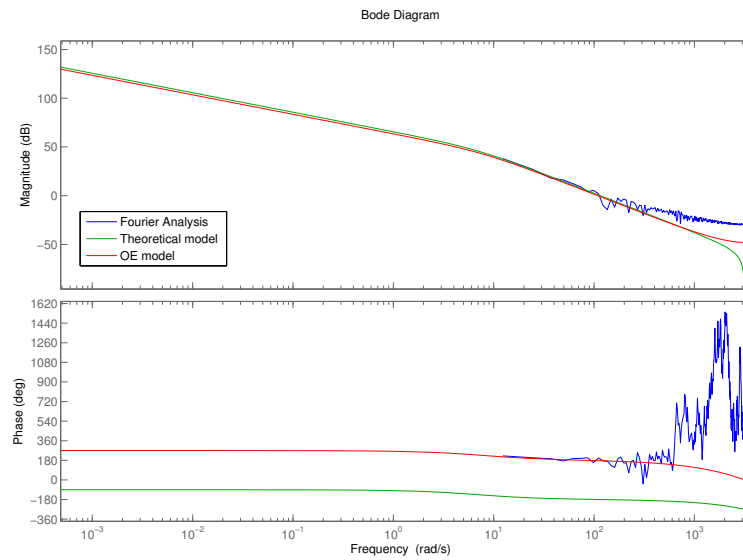


Figure 4.4: Bode diagram of the theoretical model, the identified model and the result of the Fourier analysis on the rotation system.

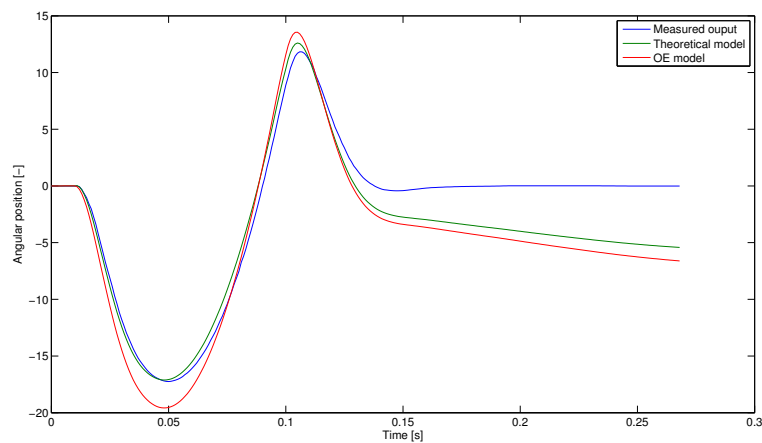


Figure 4.5: Comparison of the two identified models against measured data for a shoot (without ball).

4.1.2 Player translation system

The analysis for the translation axis can be made on a similar basis as for the rotational axis, but the following points are worth mentioning:

- The system can either be seen as a 2nd order system if the timing belt is taken to be rigid or as a 4th order system in the other case.
- The static friction is important.
- The viscous friction coefficient seems to be non-linear.

As we are trying to find the transfer function of this system, we will neglect the last two points and to have a simple model to work with for the controller design, the effect of the belt will also be neglected (future comparison with measured data justifies this approach). The Newton law for this system is similar to Equation (4.1), but we need to express the relation between the voltage and the current in the motor. Equation (1.8) from [2] gives us exactly that and becomes for the considered system Equation (4.6). We finally need the relation between the applied voltage and the set value given in term of speed. It can be easily expressed using the constants of the motor (nominal voltage and no load speed converted to rad/s): Equation (4.7).

$$I\ddot{\phi} + (M_f + K_m^2/R)\dot{\phi} = \frac{K_m}{R}u \quad (4.6)$$

$$u = \omega \frac{36}{16700 \cdot \pi/30} \quad (4.7)$$

Combining Equations (4.6) and (4.7), one gets the differential equation linking the position to the speed command given by the LabView interface.

$$I\ddot{\phi} + (M_f + K_m^2/R)\dot{\phi} = \frac{K_m}{R} \frac{36}{16700 \cdot \pi/30} \omega \quad (4.8)$$

Based on Equation (4.8), the transfer functions (continuous and discretized) are given by Equations (4.9) and (4.10), when substituting the numerical values into the discretized model. The parameters have been estimated using physical data (such as K_m and R which are given by maxonmotor) or have been adjusted against a step response (Figure 4.7). The final values are $J = 1.6794 \cdot 10^{-5} [kgm^2]$, $M_f = 0.0008 [Nm s]$, $R = 0.21 [\Omega]$ and $K_m = 0.0205 [Nm/A]$.

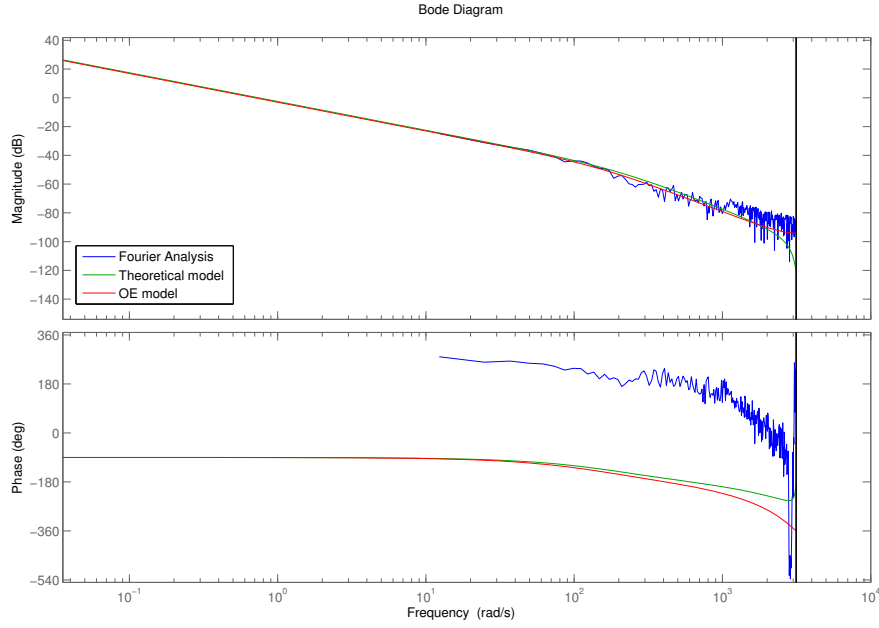


Figure 4.6: Bode diagram with the result of the Fourier Analysis, the theoretical model and the model identified by using an output error structure.

$$G_t(s) = \frac{\frac{Km}{JR} \frac{36}{16700 \cdot \pi / 30}}{s(1 + \frac{M_f + K_m^2/R}{J} s)} \quad (4.9)$$

$$G_t(z) = \frac{5.664 \cdot 10^{-5} z + 5.357 \cdot 10^{-5}}{z^2 - 1.8464z + 0.8464} \quad (4.10)$$

Following the same approach as for the rotation motor, using an output error structure a system identification with an MSL signal as excitation has been performed. The identified model is given by Equation (4.11) and the bode diagram is shown on Figure 4.6. As can be seen, the effect of the belt might only be visible at frequencies higher then approximately 1000 rad/s , but it does not seem to be of great importance.

$$G_{t_{oe}}(z) = \frac{1.447 \cdot 10^{-5} z + 8.672 \cdot 10^{-5}}{z^2 - 1.856z + 0.856} \quad (4.11)$$

Both models have be compared to measured data (Figure 4.7) and they both given good results. The shift in the measured data is certainly due to some static friction that is per definition, not simulated by these models.

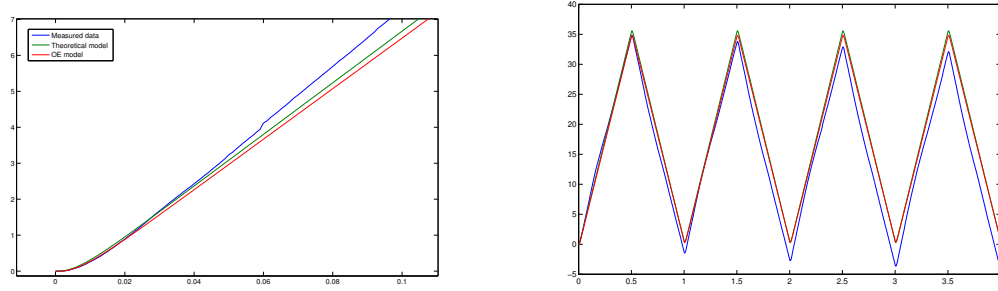


Figure 4.7: Response of the translation axis to a sequence of steps and comparison with two models

4.2 Controller design

The controller implemented in the LabView interface is based on an augmented state-space representation. For each motor, LabView calculates a column-vector $x = [x \quad \dot{x} \quad i]^T$, where i is the value of the integrator. The state vector is constructed as shown in Equation (4.12). The coefficient of the controller are thus a line-vector K and the applied command is then given by $u = -Kx$. In the LabView interface, these coefficients can be set independently for each motor (and bar), but note that you need to enter the values of $-K^{-1}$.

$$x(k) = \begin{bmatrix} \theta(k) - \theta_c(k) \\ \dot{\theta}(k) \\ i(k-1) - T_s(\theta(k) - \theta_c(k)) \end{bmatrix} \quad (4.12)$$

Considering two 2nd order systems (with their states being position and speed), the coefficient of K can be seen as the coefficient of a parallel PID controller $K = [Kp \quad Kd \quad -Ki]$. The slight difference in implementation is in the derivative term. To see this, we look at the derivate contribution to the command for both implementations.

$$u_d = K_d \frac{de}{dt} = K_d \frac{d}{dt}(\theta_c - \theta) = K_d \dot{\theta}_c - K_d \dot{\theta} \quad (4.13)$$

$$u_d = -K_d \dot{\theta} \quad (4.14)$$

When, θ_c is constant the two implementations are equivalent. When θ_c changes, the derivate term in a PID tends to create jitter, which is not the case when using directly the speed. Having with this explained and demonstrated the equivalence of the chosen implementation with a

¹To be close to a PID controller the two first coefficient should be negative, but the third should be positive.

PID controller, the loop-shaping design approach is then applied.

4.2.1 Rotation axis controller

To control the movement of the system in rotation, a PD controller is chosen. The derivative time constant is adjusted so that around the cut-off frequency the slope of the frequency response is of -20 dB per decay. Doing this, we have $T_d = 0.015$. Then, setting the wanted cut-off frequency to be of $\omega_x = 200 \text{ rad/s}$ (settling time $4/\omega_x = 20 \text{ ms}$), the required K_p is $K_p = 0.7079$. In particular for the chosen implementation the values to enter are:

$$-K = [-0.7079 \quad -0.0106 \quad 0]$$

The performances are validated on Figure 4.8. The settling time is greater then expected (around 35 ms), but the overall speed is sufficient when looking a the full shoot sequence (Figure 4.5). When looking at the command given, it gets very close to 15 A and thus, for steps of greater amplitude, some saturation will occur. Depending on the needs, a softer controller might be wanted and is left for future students to design.

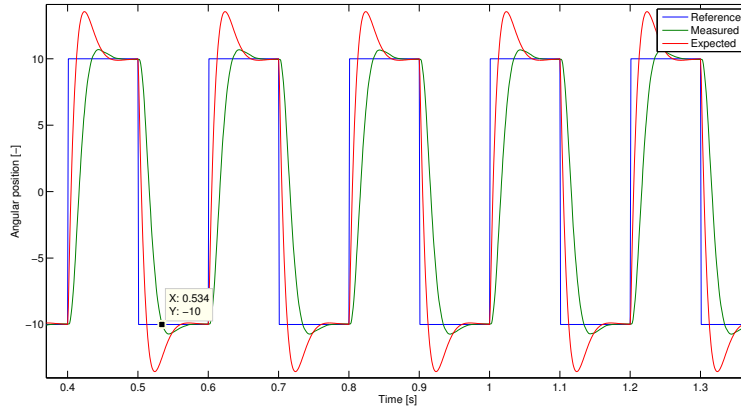


Figure 4.8: Validation of the designed controller for the rotation axis.

4.2.2 Translation axis controller

For the system in translation, a PID controller is designed. The integrator term is added to overcome some effects of the static friction. The same approach as previously is applied to get $T_d = 0.0059$ and the cut-off frequency is set at $\omega_x = 20 \text{ rad/s}$ (settling time of 200 ms), giving us $K_p = 22.3872$. Finally, the integrator time constant is chosen $T_i = 1$. In particular for the chosen implementation the values to enter are:

$$-K = [-22.3872 \quad -0.1321 \quad 22.3872]$$

The requested performances are assessed on Figure 4.9. The translation axis does behave almost like expected and the settling time is even better then expected. Further tests have shown that when the axis is not located at the same point (here in the middle), the overshoot that is predicted does happen. Figure 5.3 illustrates the performances of the controller when in a "real" situation. Increasing the integrator term could help to follow ramp references, but would increase the overshoot.

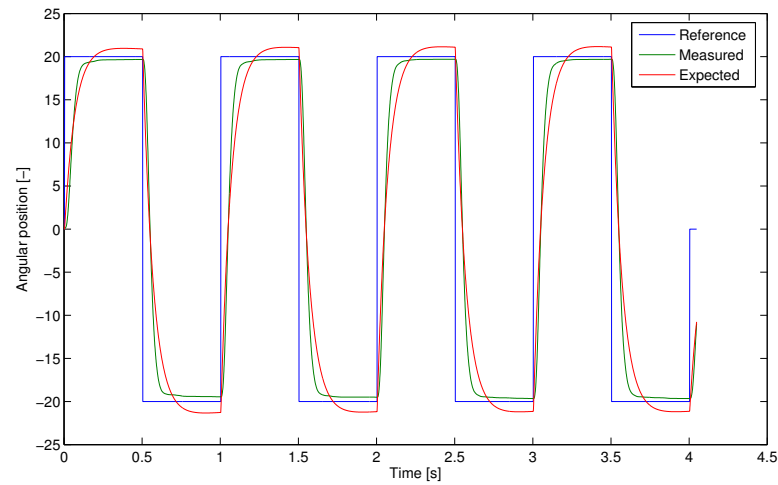


Figure 4.9: Validation of the designed controller for the translation axis.

5 Play strategies

In this final chapter, the two implemented play strategies will be described, but before getting into more details some more general sequences of the LabView interface are mentioned.

In general, the state-machine approach has been used to implement the wanted algorithms.

5.1 General sequences

5.1.1 Initialization

The initialization process is used to record the extreme positions (physical limits) of each actuator. It is run each time the LabView main VI is started. It is very similar to the initialization process used previously, but it was programmed with the state machine approach, that will not be detailed here. As suggested by Matteo in his report, after having found the maximum, the system first returns quickly to its original position before going slowly backwards to find the minimum, this in order to reduce the required time for initialization.

5.1.2 Shoot

The shoot subsequence which is used in the manual mode and in combination with the track & shoot algorithms, is composed of 4 states shown on Figure 5.1 and generates references for the rotation motor. With the controller activated, it loads the shoot and waits for the system to be "loaded" (flag that can be read by others) and for the flag "Trigger" to be set to true before moving to the next state. It then switches to open-loop control with a first stage called "Boost", which aims to start the opposite movement more gently, before moving to the next stage "Shoot" where full power is requested from the motor. After passing by the vertical position, a break command is transmitted to the motor and the flag "ended" is set so that other algorithms know that they can take back control over the rotation motor.

This subsequence is reusable in many situations and allows two execution modes: strong and

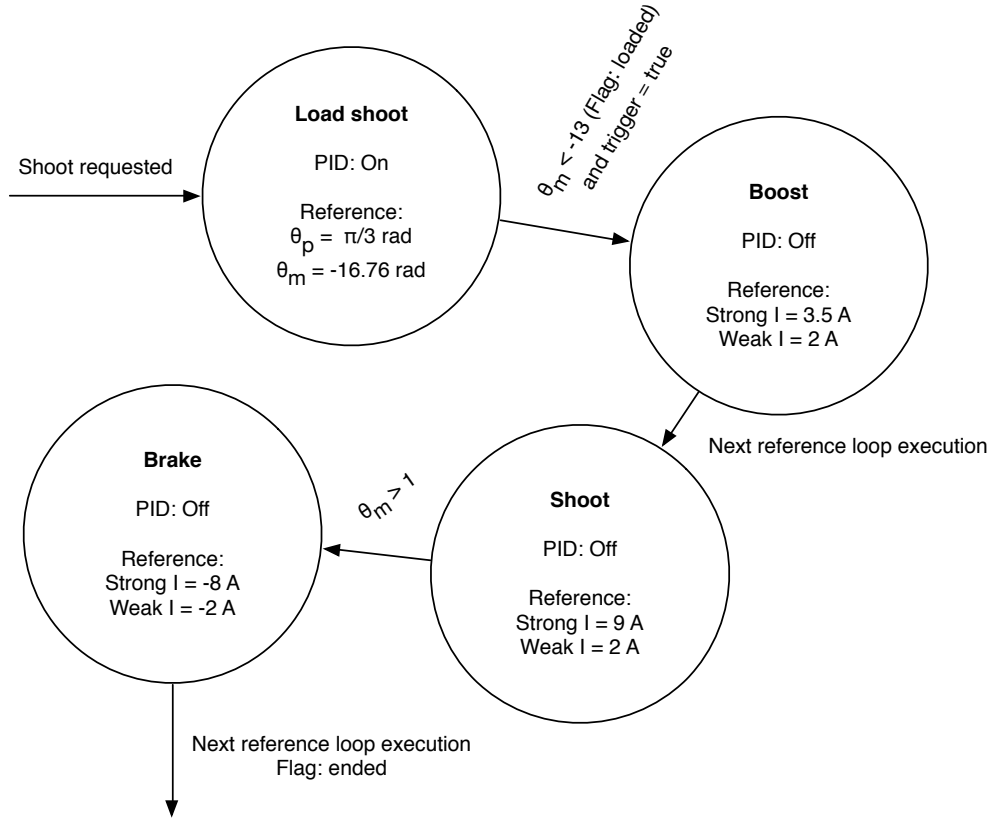


Figure 5.1: Shoot subsequence state machine representation

weak. The chosen current for each stage have been chosen experimentally and could well be refined if needed.

5.2 Implemented strategies

5.2.1 Track & shoot

One of the most simple game strategy that can be implemented is the non-collaborative – each bar is independent – track & shoot algorithm. It is simple because there is no interaction between multiple bars and the positions of the translation and rotation motor are independently calculated. The system follows the ball and shoots if the ball is within a specified threshold.

In the state machine approach, this strategy has only two states: track or shoot (Figure 5.2). In both, the system finds, if possible, the closest player and generates the reference accordingly to the actual position of the ball. If no player is within range, the players will be moved to the closest possible position. In tracking mode, the players are either vertical if the ball is in front or slightly tilted backwards if the ball is behind (enough to let the ball pass underneath).

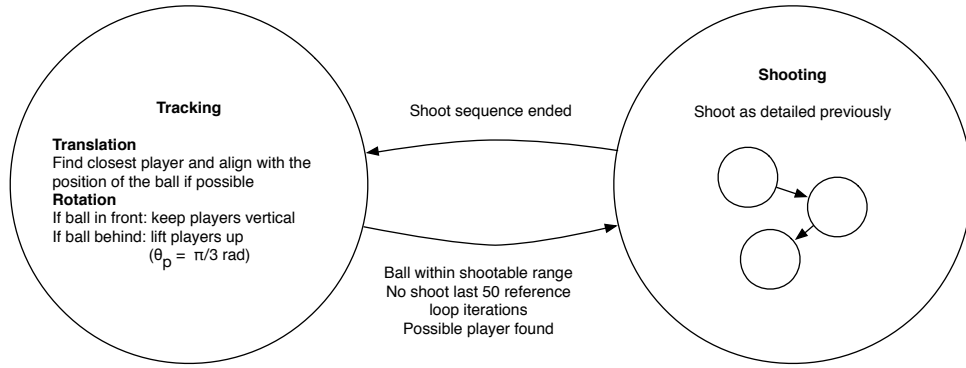


Figure 5.2: Track & shoot algorithm state machine representation

The three conditions to pass into shoot mode are: 1. the ball is between $x_{bar} + 25mm$ and $x_{bar} - 15mm$, 2. no shoot has been made within the last 50 iterations of the reference loop and 3. a player can go to the y coordinate of the ball. When the three are met the system shoots and returns to take tracking mode as soon as it ended.

To reduce the stress caused by successful step references, at each iteration of the reference loop, a small ramp is calculated to smoothen the reference. The ramp is only generated when the changes in position are smaller than $45rad$ (corresponding to half of the distance between the two players on the defense bar). The slope is calculated based on a six-step transition from the old position to the new position, but only the five last values are used. So, the first given reference is already different from the previous one and at the fifth iteration of the real-time loop the final one is used.

Figure 5.3 shows the reference value and the actual position (in mm this time) of the system, when measuring data in the track & shoot operation mode. Assuming that the position given by the camera is precise, the system is able to follow with precision (lag of less than 5mm) movements that are not very fast (approx. $1m/s$). The lag increases with speed up to 20 – 30mm. This could be improved by optimizing the controller, but also by increasing the frame rate of the camera.

Other improvements could be made by integrating the speed of the ball (not used now) to predict the position of the ball at the level of the considered bar. There are some drawbacks: if the ball hits a player and changes its trajectory, the predicted position could change massively. Plus, as speed is calculated by numerical derivation, the system becomes very sensitive to the precision of the camera and its algorithm.

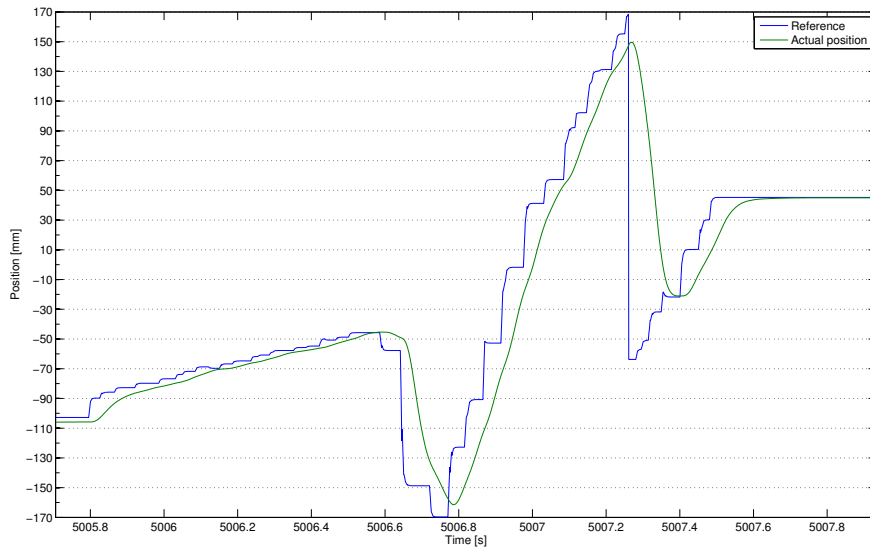


Figure 5.3: Track & shoot sequence when looking at the translation motor comparing the reference and the actual position

5.2.2 Collaborative track & shoot

The collaborative track & shoot algorithm is very close to the previously developed strategy. It also uses the same states.

The difference is in the position of the bars that are behind the closest defensive bar. All the bars that are in front of the ball and the first bar behind align with the ball and all successive bars behind shift towards the center by 40 mm each. The idea is to create a great protection zone by creating a "wall" of players.

Although being very simple, this strategy does already allow users the play against the robot with satisfactory results if the level of the humans is between low and medium.

6 Conclusion

After several weeks of intensive testing, the proposed mechanical correction seems to do its job. As partially expected though, when the players hit the ball, the additional resistive torque might cause the flexible coupling to slightly slip, because it is difficult to tighten it enough on small diameters (and the flexible coupling uses american, and not ISO metric, screws). If the issue becomes too important, I would recommend talking to the ATME workshop, which is aware of it. Some other issues with an encoder, that are unexplained so far, have arisen, but a fix made by Francis does solve the issue for now.

During this semester, clear progress has been made on the field of control and I finally was able to include the measurements of the camera into the control loop in the last week. This did not leave much time to work and test on playing algorithms. The collaborative track & shoot still does an impressive demonstration of the potential of the designed system. It was also possible to put in practice the original goal of the project: being able to play with only three players.

In general, the basis of the control setup and the LabView interface are set. Future's project should now be able to focus on enhancing the controller and developing new play strategies. They will be able to take advantage of the detailed models to simulate the effects of their imagined changes before implementing them on the automated foosball.

For the play strategies, a solid state-machine design, as well as some useful and reusable subVIs have been prepared to help them to go beyond the very simple and sometimes hysterical collaborative track & shoot algorithm. The integration, with caution, of information such as the speed of the ball, or maybe just the direction of it could help predict to optimal point to align the players with. Reimplementing the tricks of the previous semester, such as the directional shoot, would also help to make the robot behave more like an intelligent entity.

A last subject to mention is security. With the redesign, some software securities implemented before (such as the edge security) have been removed to push the performance of the system. To compensate, the references generated are strictly controlled and cannot be greater than

Chapter 6. Conclusion

the extreme positions. With the translation controllers presenting very little overshoot, this guarantees that the system won't hit the springs of the bar to roughly, unless there is a software failure. The springs on the considered foosball should in any case, limit the damages. In general, caution is required when the system is operating. The high torques and the electrical power available are significant and could led to serious injuries. Therefore, I recommend that only people well aware of the behavior of the system use it.

Acknowledgments

As final remarks, I would like to express my sincere gratitude to Dr. Christophe Salzmann for his time, support and expertise in LabView programming. My sincere thanks go to the two assistants: Milan Korda and Tomasz Gorecki for their support and enthusiasm and to Francis Tschantz for his practical support. I would like to mention Dr. Alireza Karimi for looking with me at some identification issues and Dr. Philippe Müllhaupt and David Ingram for brainstorming with me. I would like also to thank the Automatic control Laboratory and Prof. Colin Jones for letting students work on such projects.

Lausanne, December 10th 2014

A Mechanical parts order

The parts that needed to be ordered to fix the actual system and to build a 2nd actuator are listed in the tables below. As some parts were given to the lab by the ATME workshop or were left over by some other project, they don't appear in these tables, but can be found on the assembly plan (Appendix C). The parts used to create a structure for the 2nd actuator are listed in Table A.2.

Table A.1: Ordered mechanical parts

Distributor	Part number	Description	Quantity
Mädler	60151806	Metal Bellow Couplings MBK, short version	2
Mädler	6001-2Z	Deep groove bearing Din=12	2
Mädler	62341600	Shaft Collars - Double-Split, Steel	2
Mädler	16641600	Pulley 36 AT5/14-2	1
Mädler	16682200	Timing Belt 25 AT5/1050	1
MiSUMi	SSEBL16G-567	Linear Guide L=567	1

Appendix A. Mechanical parts order

Table A.2: Ordered parts for the structure (from item24)

Part number	Description	Quantity
0.0.370.03	Profile 5 20x20 natural 20x20x520	2
0.0.370.03	Profile 5 20x20 natural 20x20x100	4
0.0.370.03	Profile 5 20x20 natural 20x20x308	2
0.0.370.03	Profile 5 20x20 natural 20x20x336	2
0.0.370.03	Profile 5 20x20 natural 20x20x70	4
0.0.437.75	Profile 5 40x20 2N, natural 40x20x100	1
0.0.370.09	Cap 5 20x20, black	10
0.0.464.39	Hinge 5 20x20	4
0.0.370.01	T-slot nut 5 St M5, Zn	10
0.0.391.60	Automatic-Fastening Sets 5, Zn	24
0.0.370.08	Standards-Fastening Sets 5, Zn	6
0.0.612.79	Angle Bracket V 5 20 Zn	2
0.0.437.75	Profile 5 20x20 natural	2

B LabView interface manual

This appendix aims to give a short walkthrough the usage of the 3rd version of the LabView controller, also trying to explain where modifications can be made. Table B.1 lists all VIs contained within.

To use the automated foosball, the user should first make sure that all power supplies are switched on. He can then open the Main VI and will be presented an interface looking like Figure B.1. There, he can set all sorts of parameters ranging from the sampling rate, to the definition of the controllers through the acquisition channels. As a convention when defining the bars, they should be entered sorted and starting with the goalkeeper. Make sure that the device array, the counter arrays, the bar definition and controller arrays have the same number of elements and are sorted the same way.

To start the automated foosball, there should be no ball on the playground and when all setup parameters have been controlled, the main VI can be started. The system will first operate an initialization process to get the extreme positions. Please note that the system expects the player to be vertical before it is turned on.

To change to operation mode, the user can move to the next tab "Command & Display" (Figure B.2). On the left, he can follow the evolutions of different variables of all bars (for performance reasons the display should be turn off when not needed using the button below). The drop-down menu on the right is controlling the operation mode of the automated foosball.

To stop the VI, please use the STOP bouton of the user interface. This makes sure that all acquisition channels are correctly closed and the camera disconnected.

Appendix B. LabView interface manual

Table B.1: List of all LabView VIs and their description

VI name	Description
Controller	Controller implementation: calculates the command with a given controller and current state
DAQ_End	Writes 0 values to all outputs and closes all opened acquisition channels
DAQ_Init	Opens all required acquisition channels
gBallPosition	Global variable containing the position of the ball
gController	Global variable containing the definition of the controllers for each bar
gMode	Global variable containing the desired operation mode
gParams	Global variable containing the parameters
gRef	Global variable containing the generated references for each bar
Main	User interface and main VI
Prepare_State	Generates a state vector based on the acquired position (calculates the speed)
PrepareForGraph	Reorganizes the data in order to be displayed in a graph
ReadDAQ	Reads all counters (position)
RealTime	Real-Time loop
Saturation	Prepares the command for the WriteDAQ task
Shoot	Shoot state machine
ToTranslationRef	Finds the closest possible player with respect to the position of the ball
TrackShoot	Implementation of the track & shoot algorithm
TrackShootCollab	Implementation of the collaborative track & shoot algorithm
WriteDAQ	Writes all analog outputs
WriteEnable	Writes all digital outputs

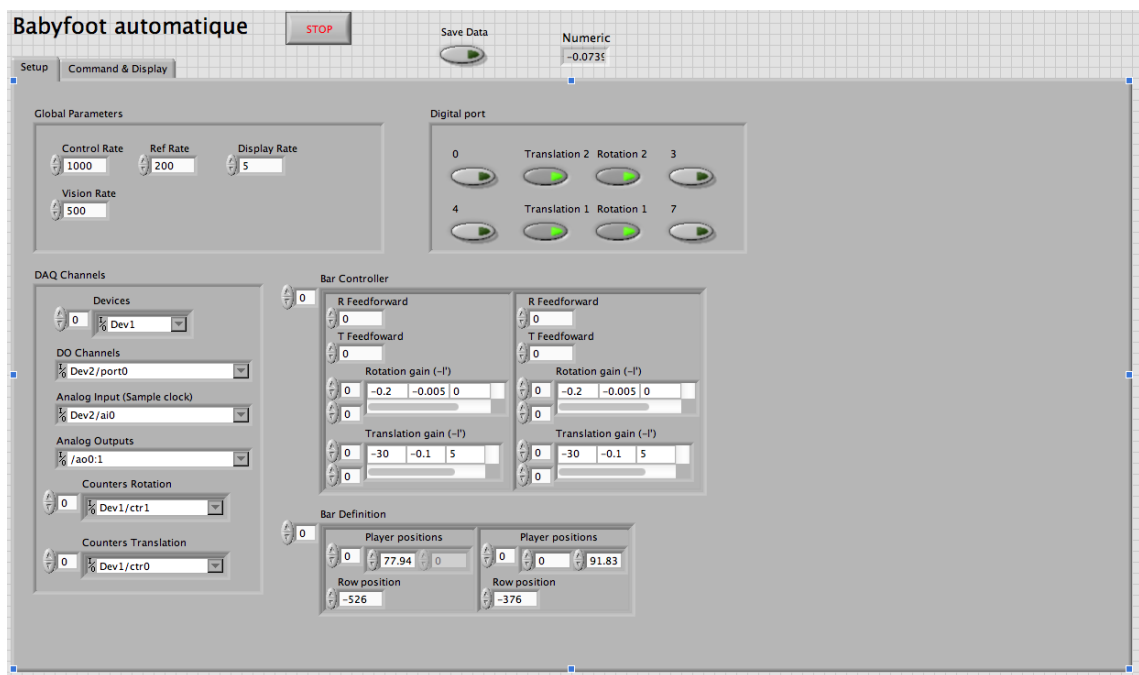


Figure B.1: Main VI setup interface

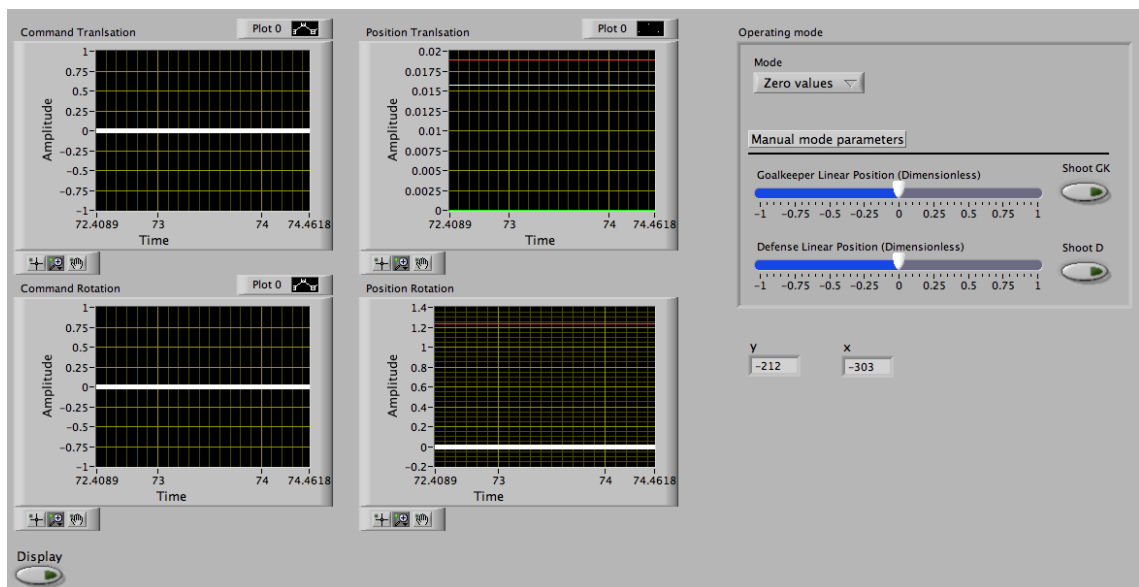
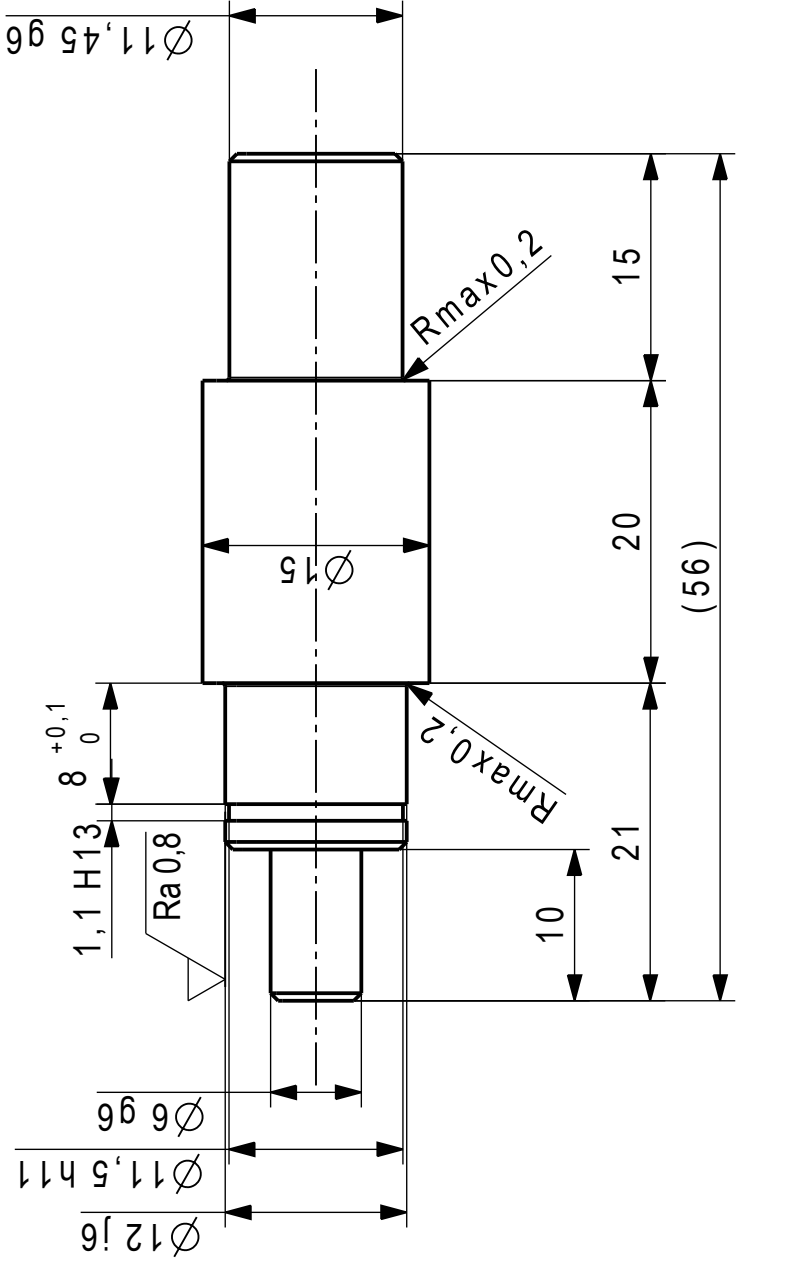


Figure B.2: Main VI control interface

C Drawings

13-LACO-CP-02
Cyril Picard
079 522 58 91
Projet Babyfoot
1 pièce

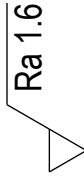


Chanfreins non cotés : $45^{\circ} \times 0,5$
Tolérances générales:
NF EN 22768 - fH
(ISO 2768 - fH)

Mod.	Mod.	Dessiné	30.09.2013	CYRIL	Echelle	2:1
		Contrôlé				
		Conf aux norm				
		Bon pour exéc.				
		N° de commande				
Sans nomenclature séparée	<input type="checkbox"/>	Origine		Format	N° feuilles	Feuille N°
Nomenclature sép de même N°	<input type="checkbox"/>	Remplace		A4	1	1
Nomenclature sép de N° diff	<input type="checkbox"/>					
Dénomination		AXE TRANSMISSION				
		N° de dessin				

A horizontal number line with tick marks at each integer from 1 to 8. The numbers 1, 2, 3, 4, 5, 6, 7, and 8 are labeled below the line.

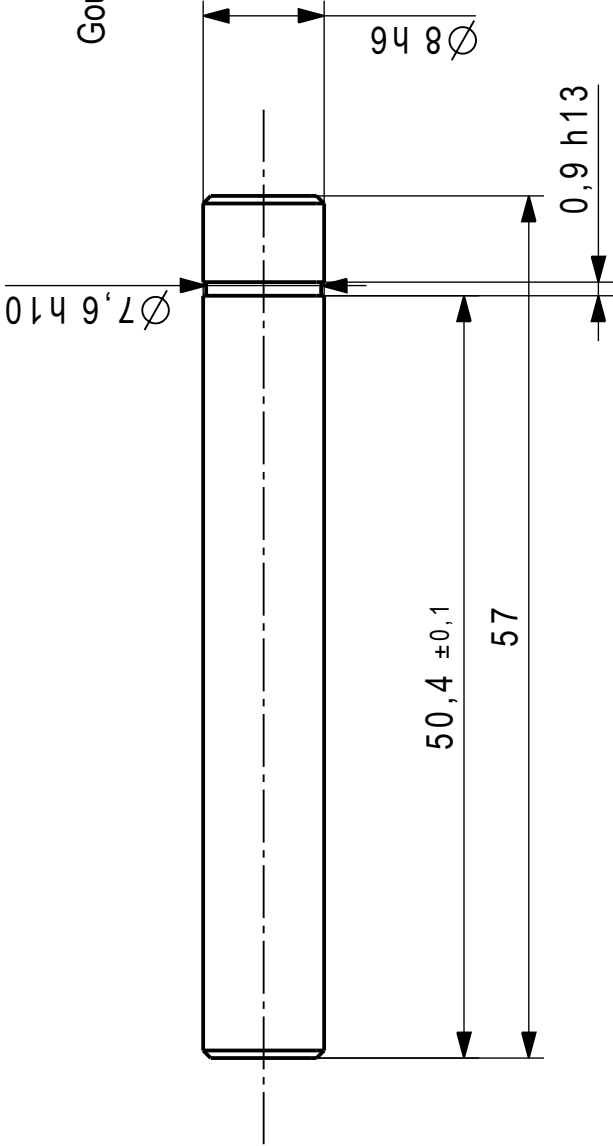
A	B	C	D	E	F
1	2	3	4	5	6
7	8	9	10	11	12
13	14	15	16	17	18
19	20	21	22	23	24
25	26	27	28	29	30
31	32	33	34	35	36
37	38	39	40	41	42
43	44	45	46	47	48
49	50	51	52	53	54
55	56	57	58	59	60
61	62	63	64	65	66
67	68	69	70	71	72
73	74	75	76	77	78
79	80	81	82	83	84
85	86	87	88	89	90
91	92	93	94	95	96
97	98	99	100	101	102
103	104	105	106	107	108
109	110	111	112	113	114
115	116	117	118	119	120
121	122	123	124	125	126
127	128	129	130	131	132
133	134	135	136	137	138
139	140	141	142	143	144
145	146	147	148	149	150
151	152	153	154	155	156
157	158	159	160	161	162
163	164	165	166	167	168
169	170	171	172	173	174
175	176	177	178	179	180
181	182	183	184	185	186
187	188	189	190	191	192
193	194	195	196	197	198
199	200	201	202	203	204
205	206	207	208	209	210
211	212	213	214	215	216
217	218	219	220	221	222
223	224	225	226	227	228
229	230	231	232	233	234
235	236	237	238	239	240
241	242	243	244	245	246
247	248	249	250	251	252
253	254	255	256	257	258
259	260	261	262	263	264
265	266	267	268	269	270
271	272	273	274	275	276
277	278	279	280	281	282
283	284	285	286	287	288
289	290	291	292	293	294
295	296	297	298	299	300
301	302	303	304	305	306
307	308	309	310	311	312
313	314	315	316	317	318
319	320	321	322	323	324
325	326	327	328	329	330
331	332	333	334	335	336
337	338	339	340	341	342
343	344	345	346	347	348
349	350	351	352	353	354
355	356	357	358	359	360
361	362	363	364	365	366
367	368	369	370	371	372
373	374	375	376	377	378
379	380	381	382	383	384
385	386	387	388	389	390
391	392	393	394	395	396
397	398	399	400	401	402
403	404	405	406	407	408




12345678

13-LACO-CP-02
Cyril Picard
079 522 58 91
Projet Babyfoot
1 pièce

Goupille trempée h6

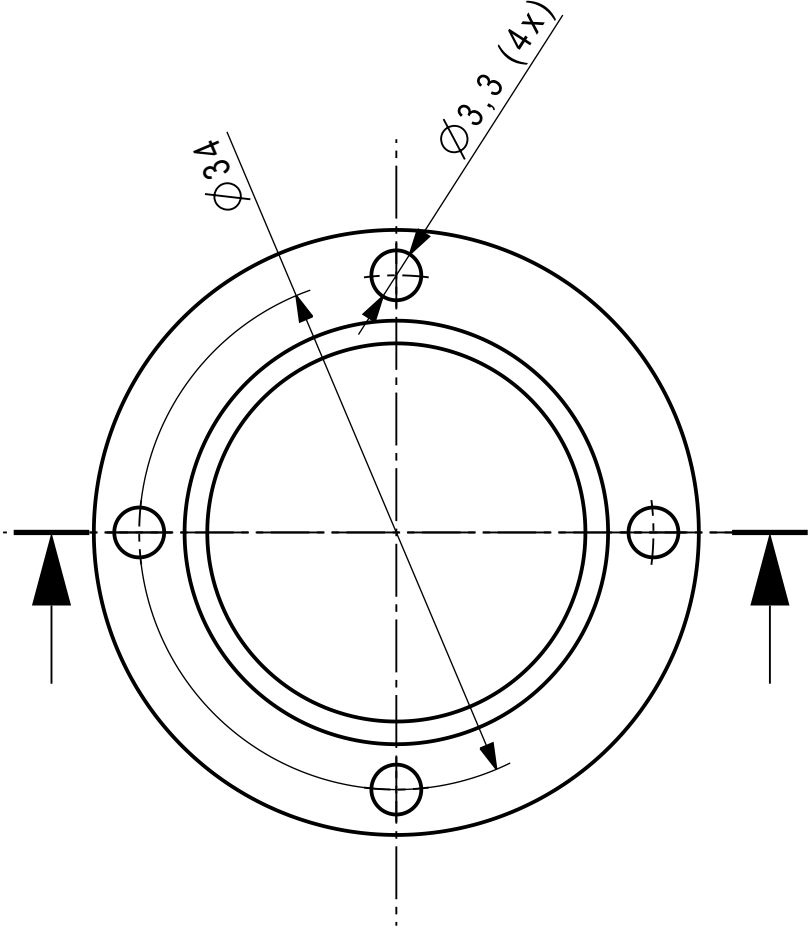


Ra 1.6

Mod.		Mod.				Dessiné	11/2/2012	Projet Babyfoot		Echelle 2:1	
						Contrôlé					
						Conf aux norm					
						Bon pour exéc.					
Sans nomenclature séparée						N° de commande			Format A4	Nb feuilles 1	Feuille N° 1
						Origine					
						Remplace					
Nomenclature sép de même N°		-						N° de dessin			
Nomenclature sép de N° diff		0 kg									
		Dénomination		Axe							

Chanfreins non cotés: 45° x 0.5
Tolérances générales:
NF EN 22768 - mH
(ISO 2768 - mH)

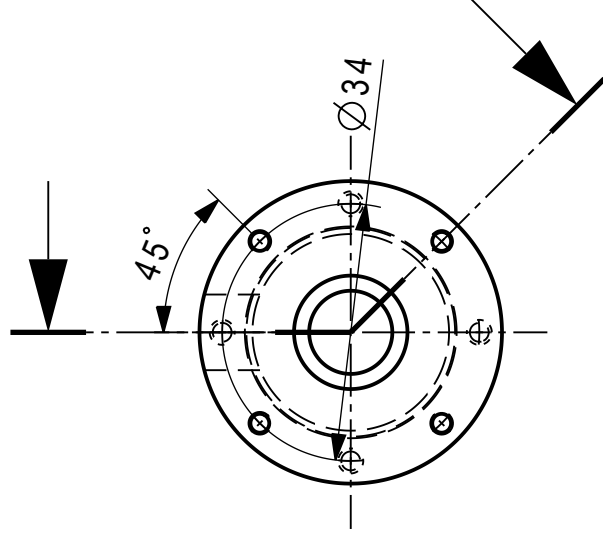
13-LACO-CP-02
Cyril Picard
079 522 58 91
Projet Babyfoot
1 pièce



Chanfreins 0,3 x 45°
Tolérances générales:
NF EN 22768 - mH
(ISO 2768 - mH)

Mod.	Mod.	Dessiné	30.09.2013	CYRIL	Echelle	2:1
		Contrôle				
		Conf aux norm				
		Bon pour exéc.				
Sans nomenclature séparée		N° de commande				
Nomenclature sép de même N°		Origine				
Nomenclature sép de N° diff		Remplace				
		Matière	Aluminium			
		Masse	0.004 kg			
Dénomination			BAGUE CYLINDRIQUE			
			Format	Nb feuilles	Feuille N°	
			A4	1	1	
			N° de dessin			

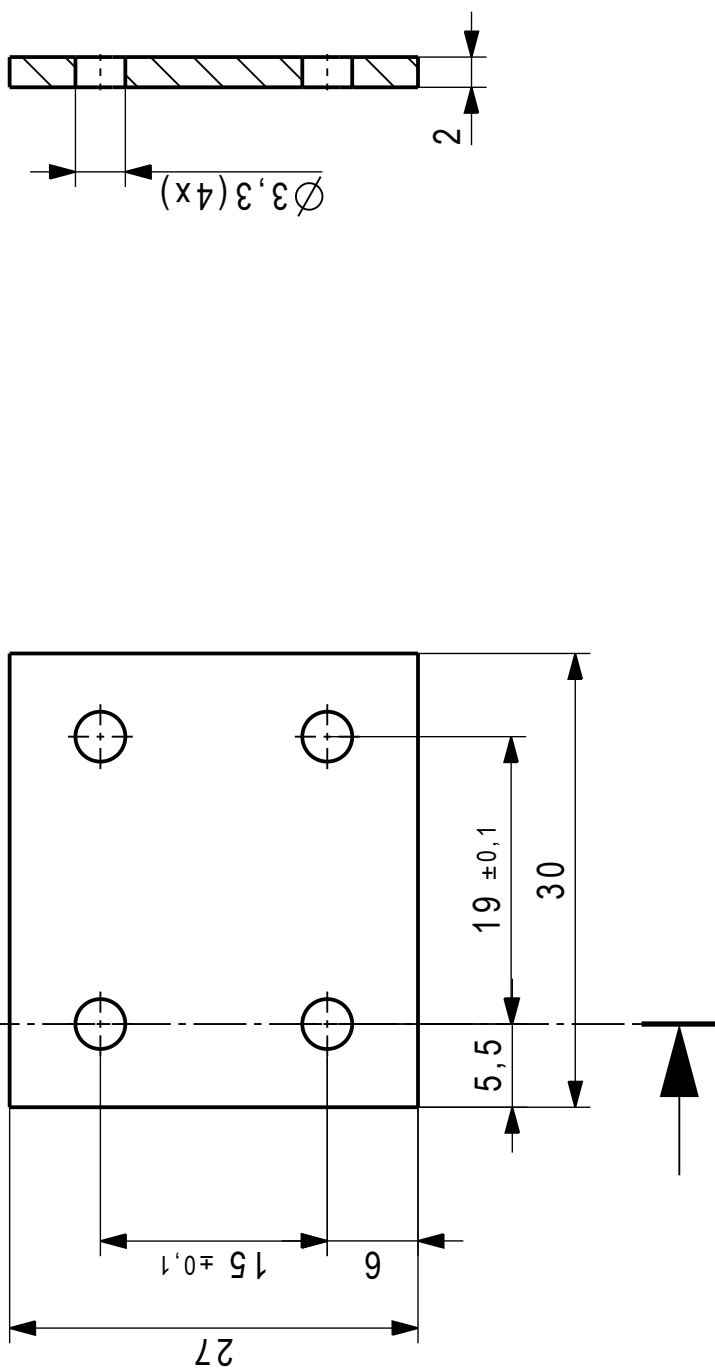
1 pièce



Tolérances générales:
NF EN 22768 - fH
(ISO 2768 - fH)

CLOCHEV2

13-LACO-CP-02
Cyril Picard
079 522 58 91
Projet Babyfoot
1 pièce



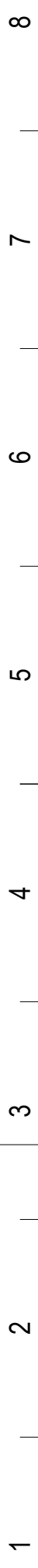
Ra 3,2

Tolérances générales:
NF EN 22768 - mH
(ISO 2768 - mH)

--	--	--	--	--	--	--	--	--	--	--	--	--	--	--	--	--	--	--	--	--	--	--	--	--	--	--	--	--	--	--	--	--	--	--	--	--	--	--	--	--	--	--	--	--	--	--	--	--	--	--	--	--	--	--	--	--	--	--	--	--	--	--	--	--	--	--	--	--	--	--	--	--	--	--	--	--	--	--	--	--	--	--	--	--	--	--	--	--	--	--	--	--	--	--	--	--	--	--	--	--	--	--	--	--	--	--	--	--	--	--	--	--	--	--	--	--	--	--	--	--	--	--	--	--	--	--	--	--	--	--	--	--	--	--	--	--	--	--	--	--	--	--	--	--	--	--	--	--	--	--	--	--	--	--	--	--	--	--	--	--	--	--	--	--	--	--	--	--	--	--	--	--	--	--	--	--	--	--	--	--	--	--	--	--	--	--	--	--	--	--	--	--	--	--	--	--	--	--	--	--	--	--	--	--	--	--	--	--	--	--	--	--	--	--	--	--	--	--	--	--	--	--	--	--	--	--	--	--	--	--	--	--	--	--	--	--	--	--	--	--	--	--	--	--	--	--	--	--	--	--	--	--	--	--	--	--	--	--	--	--	--	--	--	--	--	--	--	--	--	--	--	--	--	--	--	--	--	--	--	--	--	--	--	--	--	--	--	--	--	--	--	--	--	--	--	--	--	--	--	--	--	--	--	--	--	--	--	--	--	--	--	--	--	--	--	--	--	--	--	--	--	--	--	--	--	--	--	--	--	--	--	--	--	--	--	--	--	--	--	--	--	--	--	--	--	--	--	--	--	--	--	--	--	--	--	--	--	--	--	--	--	--	--	--	--	--	--	--	--	--	--	--	--	--	--	--	--	--	--	--	--	--	--	--	--	--	--	--	--	--	--	--	--	--	--	--	--	--	--	--	--	--	--	--	--	--	--	--	--	--	--	--	--	--	--	--	--	--	--	--	--	--	--	--	--	--	--	--	--	--	--	--	--	--	--	--	--	--	--	--	--	--	--	--	--	--	--	--	--	--	--	--	--	--	--	--	--	--	--	--	--	--	--	--	--	--	--	--	--	--	--	--	--	--	--	--	--	--	--	--	--	--	--	--	--	--	--	--	--	--	--	--	--	--	--	--	--	--	--	--	--	--	--	--	--	--	--	--	--	--	--	--	--	--	--	--	--	--	--	--	--	--	--	--	--	--	--	--	--	--	--	--	--	--	--	--	--	--	--	--	--	--	--	--	--	--	--	--	--	--	--	--	--	--	--	--	--	--	--	--	--	--	--	--	--	--	--	--	--	--	--	--	--	--	--	--	--	--	--	--	--	--	--	--	--	--	--	--	--	--	--	--	--	--	--	--	--	--	--	--	--	--	--	--	--	--	--	--	--	--	--	--	--	--	--	--	--	--	--	--	--	--	--	--	--	--	--	--	--	--	--	--	--	--	--	--	--	--	--	--	--	--	--	--	--	--	--	--	--	--	--	--	--	--	--	--	--	--	--	--	--	--	--	--	--	--	--	--	--	--	--	--	--	--	--	--	--	--	--	--	--	--	--	--	--	--	--	--	--	--	--	--	--	--	--	--	--	--	--	--	--	--	--	--	--	--	--	--	--	--	--	--	--	--	--	--	--	--	--	--	--	--	--	--	--	--	--	--	--	--	--	--	--	--	--	--	--	--	--	--	--	--	--	--	--	--	--	--	--	--	--	--	--	--	--	--	--	--	--	--	--	--	--	--	--	--	--	--	--	--	--	--	--	--	--	--	--	--	--	--	--	--	--	--	--	--	--	--	--	--	--	--	--	--	--	--	--	--	--	--	--	--	--	--	--	--	--	--	--	--	--	--	--	--	--	--	--	--	--	--	--	--	--	--	--	--	--	--	--	--	--	--	--	--	--	--	--	--	--	--	--	--	--	--	--	--	--	--	--	--	--	--	--	--	--	--	--	--	--	--	--	--	--	--	--	--	--	--	--	--	--	--	--	--	--	--	--	--	--	--	--	--	--	--	--	--	--	--	--	--	--	--	--	--	--	--	--	--	--	--	--	--	--	--	--	--	--	--	--	--	--	--	--	--	--	--	--	--	--	--	--	--	--	--	--	--	--	--	--	--	--	--	--	--	--	--	--	--	--	--	--	--	--	--	--	--	--	--	--	--	--	--	--	--	--	--	--	--	--	--	--	--	--	--	--	--	--	--	--	--	--	--	--	--	--	--	--	--	--	--	--	--	--	--	--	--	--	--	--	--	--	--	--	--	--	--	--	--	--	--	--	--	--	--	--	--	--	--	--	--	--	--	--	--	--	--	--	--	--	--	--	--	--	--	--	--	--	--	--	--	--	--	--	--	--	--	--	--	--	--	--	--	--	--	--	--	--	--	--	--	--	--	--	--	--	--	--	--	--	--	--	--	--	--	--	--	--	--	--	--	--	--	--	--	--	--	--	--	--	--	--	--	--	--	--	--	--	--	--	--	--	--	--	--	--	--	--	--	--	--	--	--	--	--	--	--	--	--	--	--	--	--	--	--	--	--	--	--	--	--	--	--	--	--	--	--	--	--	--	--	--	--	--	--	--	--	--	--	--	--	--	--	--	--	--	--	--	--	--	--	--	--	--	--	--	--	--	--	--	--	--	--	--	--	--	--	--	--	--	--	--	--	--	--	--	--	--	--	--	--	--	--	--	--	--	--	--	--	--	--	--	--	--	--	--	--	--	--	--	--	--	--	--	--	--	--	--	--	--	--	--	--	--	--	--	--	--	--	--	--	--	--	--	--	--	--	--	--	--	--	--	--	--	--	--	--	--	--	--	--	--	--	--	--	--	--	--	--	--	--	--	--	--	--	--	--	--	--	--	--	--	--	--	--	--	--	--	--	--	--	--	--	--	--	--	--	--	--	--	--	--	--	--	--	--	--	--	--	--	--	--	--	--	--	--	--	--	--	--	--	--	--	--	--	--	--	--	--	--	--	--	--	--	--	--	--	--	--	--	--	--	--	--	--	--	--	--	--	--	--	--	--	--	--	--	--	--	--	--	--	--	--	--	--	--	--	--	--	--	--	--	--	--	--	--	--	--	--	--	--	--	--	--	--	--	--	--	--	--	--	--	--	--	--	--	--	--	--	--	--	--	--	--	--	--	--	--	--	--	--	--	--	--	--	--	--	--	--	--	--	--	--	--	--	--	--	--	--	--	--	--	--	--	--	--	--	--	--	--	--	--	--	--	--	--	--	--	--	--	--	--	--	--	--	--	--	--	--	--	--	--	--	--	--	--	--	--	--	--	--	--	--	--	--	--	--	--	--	--	--	--	--	--	--	--	--	--	--	--	--	--	--	--	--	--	--	--	--	--	--	--	--	--	--	--	--	--	--	--	--	--	--	--	--	--	--	--	--	--	--	--	--	--	--	--	--	--	--	--	--	--	--	--	--	--	--	--	--	--	--	--	--	--	--	--	--	--

A horizontal number line with tick marks at each integer from 1 to 8. The numbers 1, 2, 3, 4, 5, 6, 7, and 8 are labeled below the line.

A horizontal number line with tick marks at each integer from 1 to 8. The numbers 1, 2, 3, 4, 5, 6, 7, and 8 are labeled below the line.

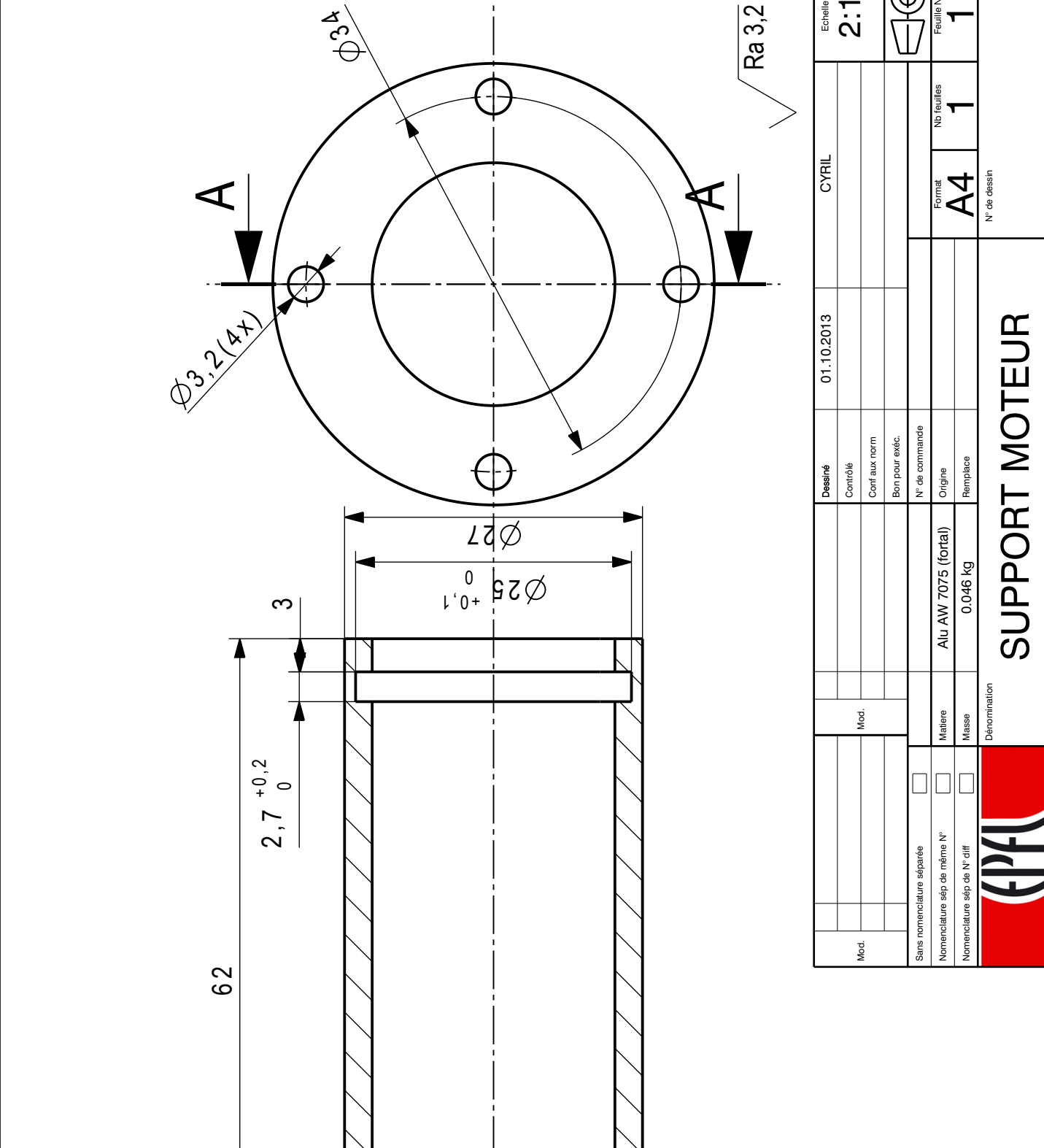


A horizontal number line with tick marks at each integer from 1 to 8. The numbers 1, 2, 3, 4, 5, 6, 7, and 8 are labeled below the line.

A horizontal number line with tick marks at each integer from 1 to 8. The numbers 1, 2, 3, 4, 5, 6, 7, and 8 are labeled below the line.

A horizontal number line with tick marks at each integer from 1 to 8. The numbers 1, 2, 3, 4, 5, 6, 7, and 8 are labeled below the line.

A horizontal number line with tick marks at each integer from 1 to 8. The numbers 1, 2, 3, 4, 5, 6, 7, and 8 are labeled below the line.



SUPPORT MOTEUR

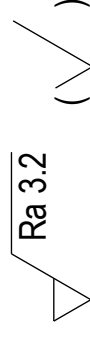
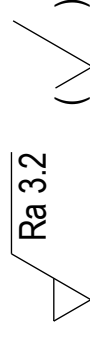
1 pièce



dessin

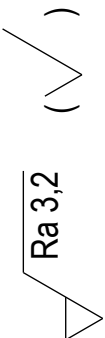
Tendeur


1 pièce



Chanfrein 45° x 0.5
Tolérances générales:
NF EN 22768 - mH
(ISO 2768-mH)

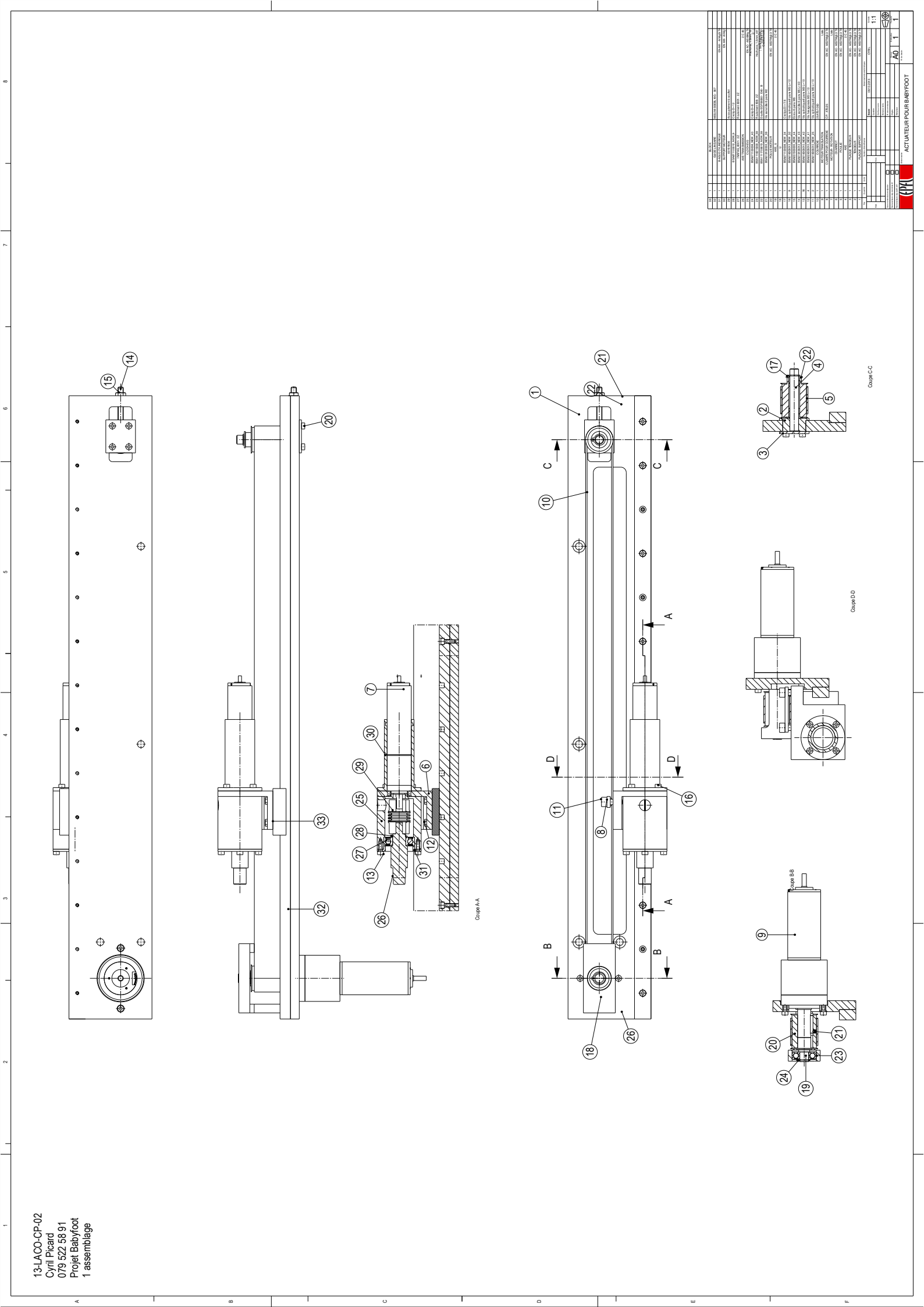
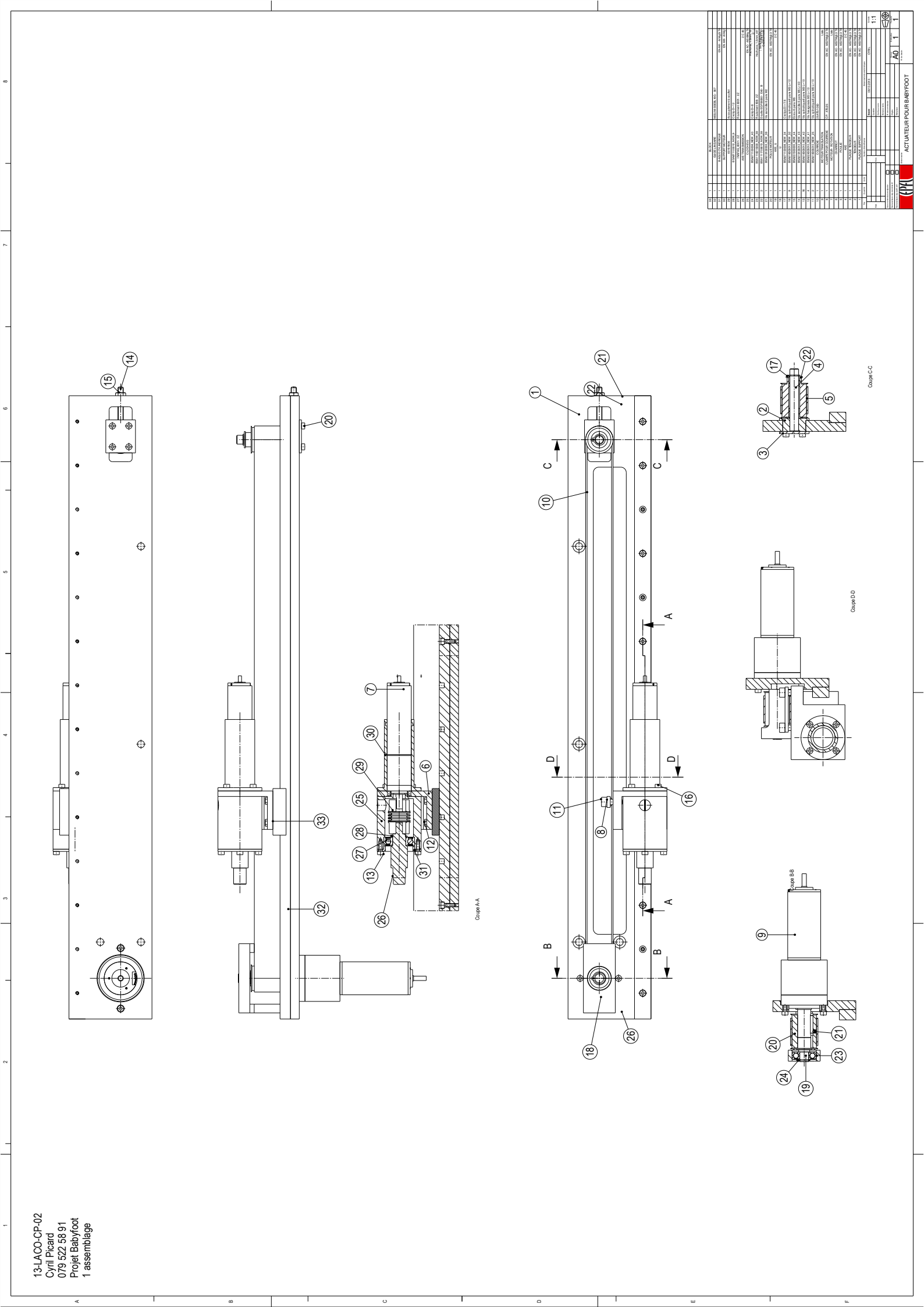
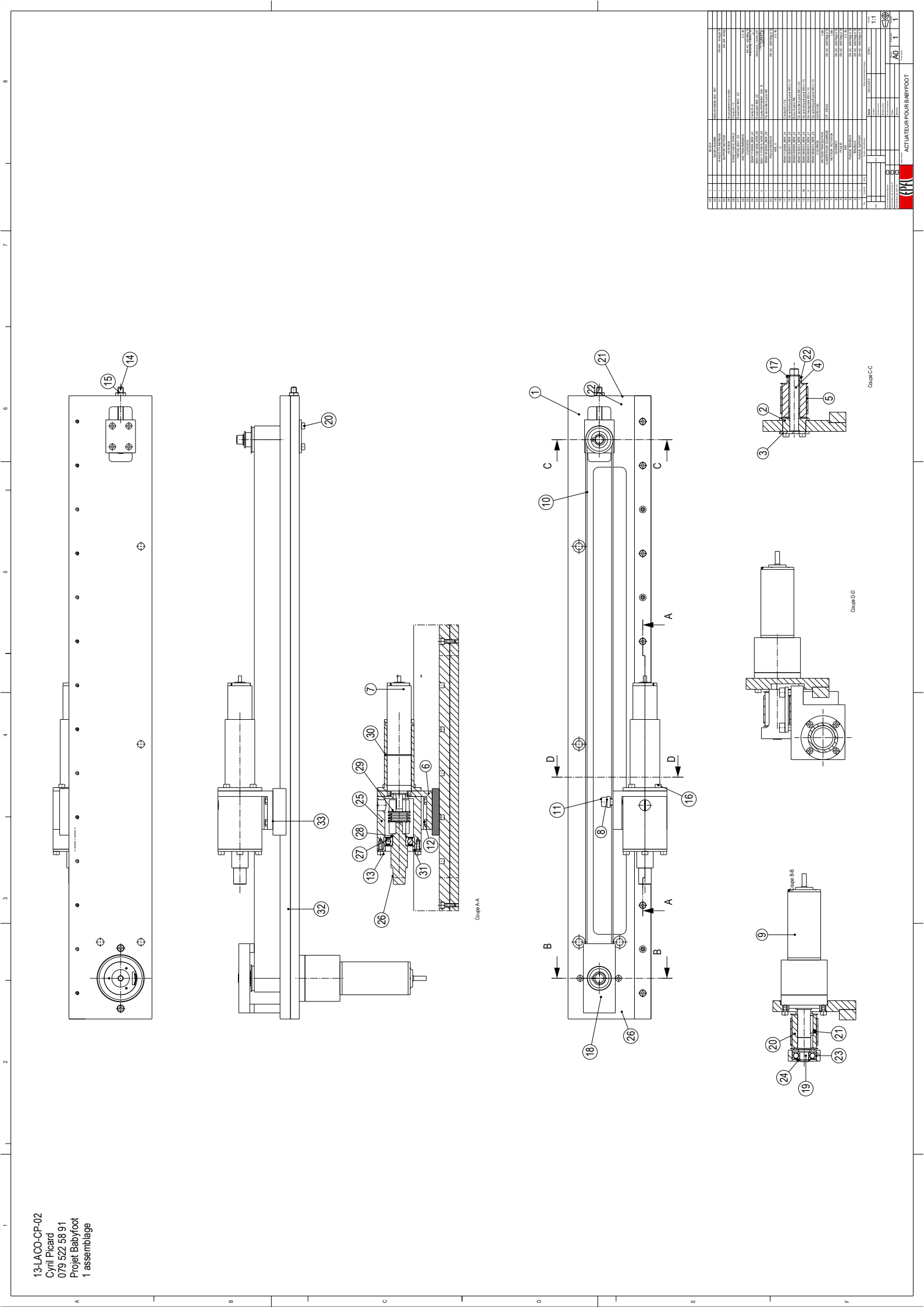
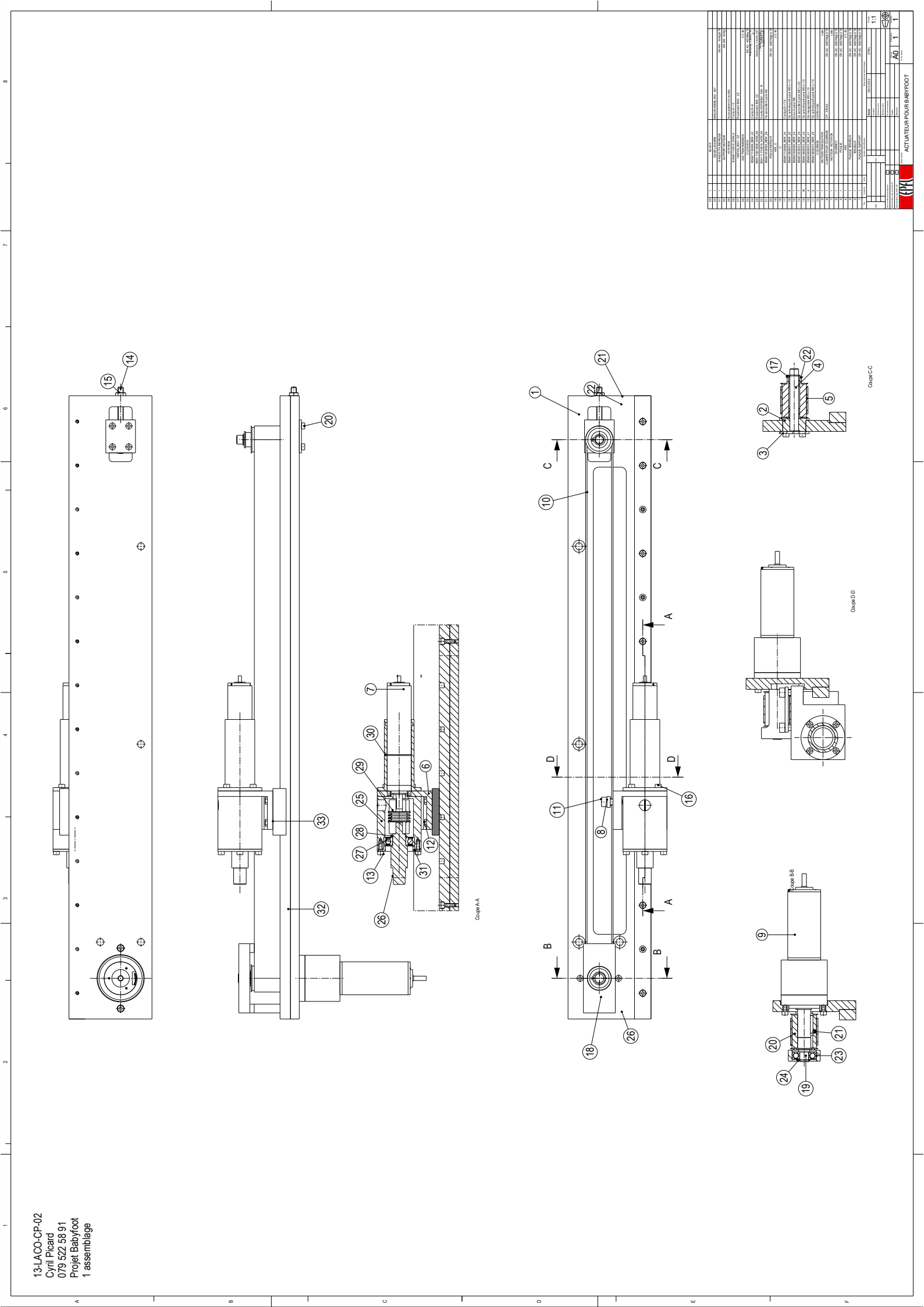
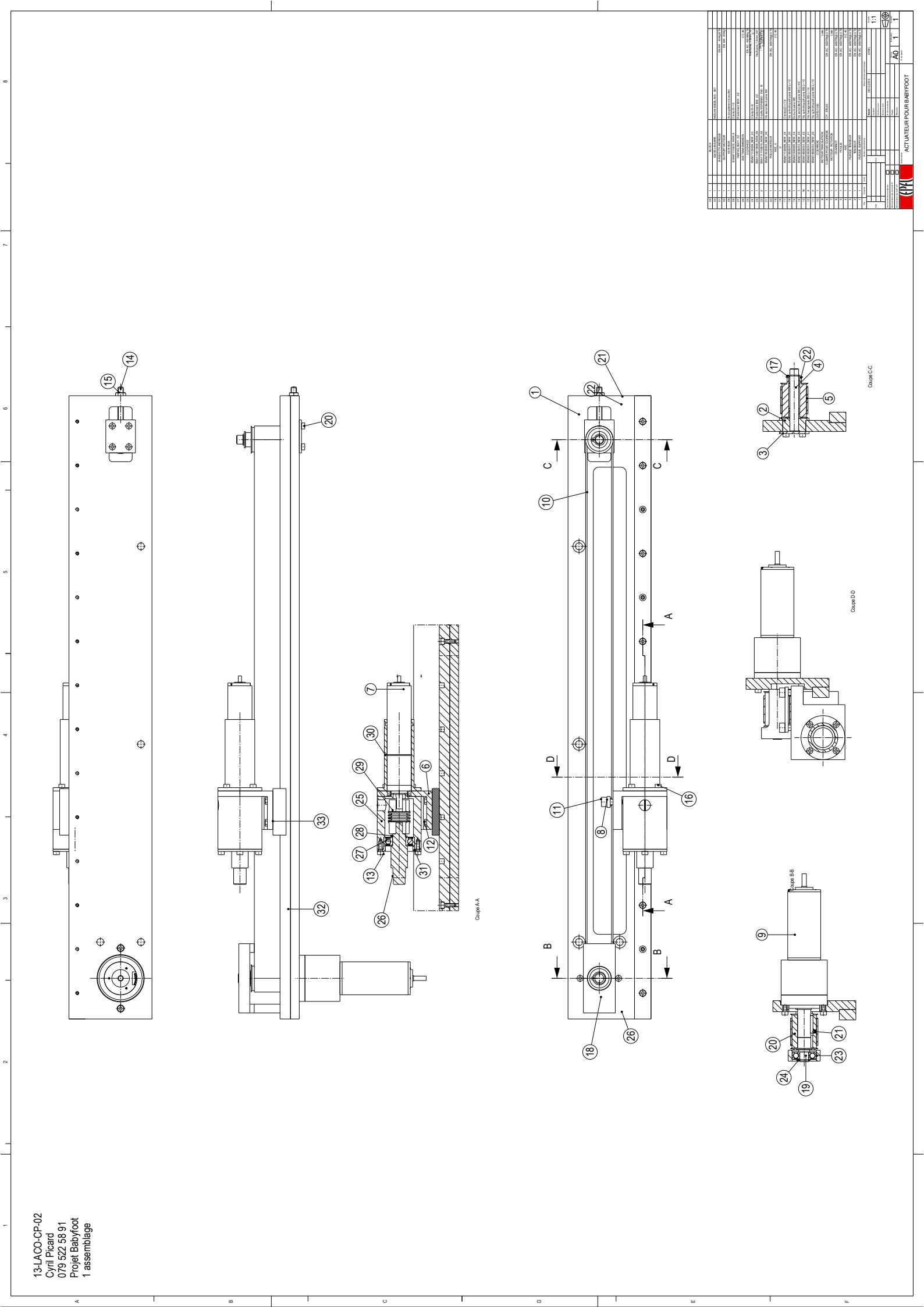
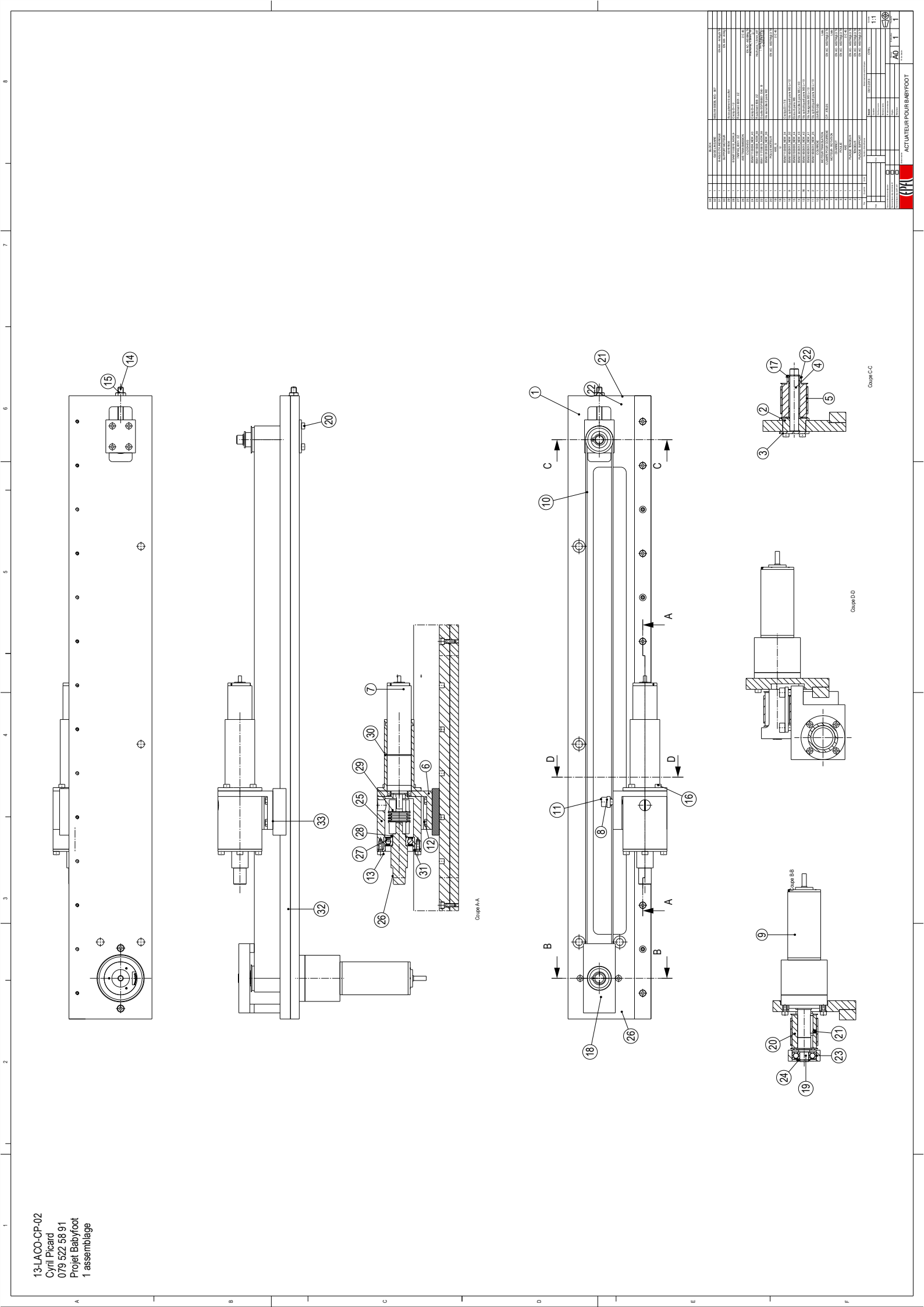
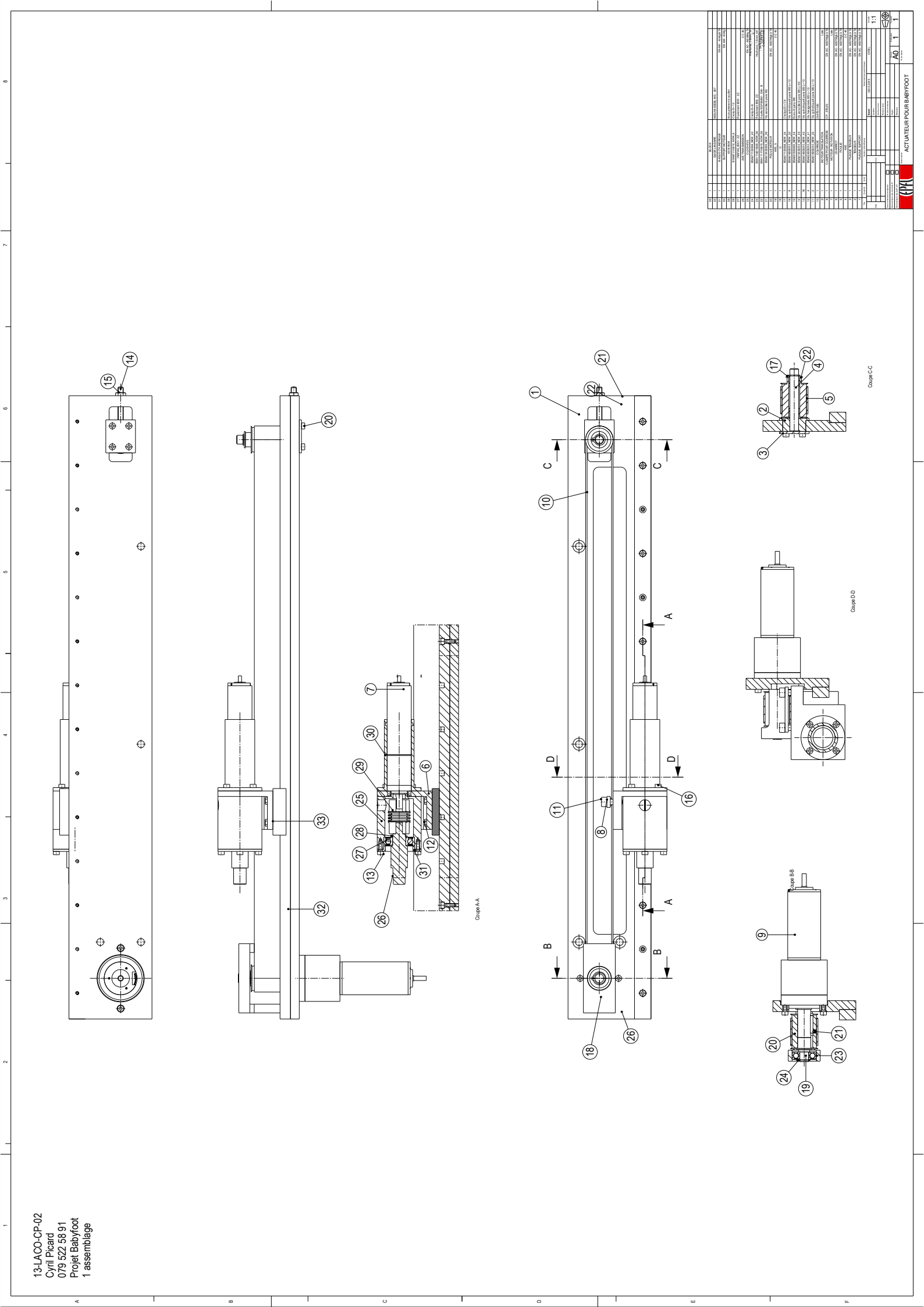
1 pièce



Mod.					Dessiné	09/10/2013	CYRIL	Echelle 1:1
					Contrôle			
					Conf aux norm			
					Bon pour exéc.			
Sans nomenclature séparée					N° de commande			
Nomenclature sép de même N°					Origine		Format A4	
Nomenclature sép de N° diff					Remplace		Nb feuilles 1	
		Dénomination			N° de dessin			
		Charriot						

PLAQUE SUPPORT

N° de dessin

[illegible][illegible][illegible][illegible][illegible]

Bibliography

- [1] Chemist Dominique Bonvin and Electrical engineer Alireza Karimi. *Identification de systèmes dynamiques*. EPFL, Lausanne, octobre 2005 edition, 2005.
- [2] Electrical engineer Roland Longchamp. *Commande numérique de systèmes dynamiques : cours d'automatique*. Presses polytechniques et universitaires romandes, Lausanne, 3e éd., entièrement revue et augm. edition, 2010.